Protein markers of oxidative stress damage: Applications to experimental research and effects of fatty acids

Trygve Danielsen

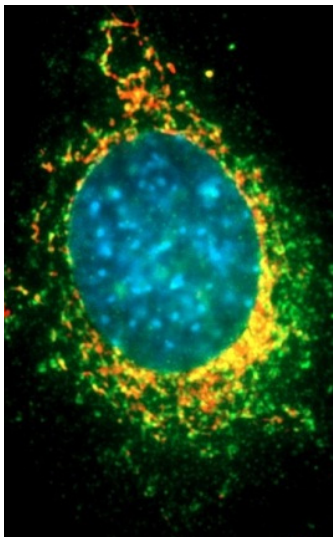

Master Thesis in Toxicology

Department of Biosciences

Faculty of Mathematics and Natural Sciences

University of Oslo

April 2015

Acknowledgement

This master thesis was done at the Department of Chemicals and Radiation, Division of Environmental Medicine, at the Norwegian Institute of Public Health from January 2013 to April 2015. Dr Tim Hofer was the main supervisor and Dr Birgitte Lindeman was co-supervisor. Professor Ketil Hylland was my internal supervisor at the University of Oslo.

I want to thank Tim and Birgitte for being my supervisors. I am extremely grateful for all the help that I have received, for always having time for my questions and for helping me out both in the lab and in the writing process. Your belief in me means more to me than I can describe in words.

I also want to thank the Department Director, Gunnar Brunborg for allowing me to do my thesis at your lab. I also want to thank you for giving me the opportunity to work at your lab for three months at the end of 2014. It means much to me! Thanks to all the people at MIKS, you guys are just great, being warm and welcoming for a new master student. Thanks to Nur for teaching me the ways of RNA-isolation and PCR while I was working at the department. Special thanks go to Hildegunn and Pål, Hildegunn for teaching me how to cultivate cells in a sterile manner and Pål for being a super guy to share an office with. I would have felt alone if I didn't have anyone to share my frustrations with, and also thanks for looking at my thesis and giving insightful advice. Thanks to Julie and Eivind for correcting spelling mistakes and looking through my introduction.

Thanks to all my friends and my family for being supportive and helping me out. I truly wouldn't have been able to finish this if it wasn't for you. You guys rock.

Oslo, April 2015

Trygve Danielsen

Abstract

Oxidative stress can cause damage to lipids, protein and DNA and thereby contribute to functional decline and the development of a variety of diseases. Environmental pollutants and a range of other stressors, including nutritional stress may induce reactive oxygen species that if not counterbalanced by the cells antioxidant defense systems will lead to oxidative stress. Precise and robust biological markers for oxidative damage are therefore important for mapping out the exact causes of these conditions. A variety of such markers have been established, including lipid peroxidation generated malondialdehyde and DNA oxidation markers such as 8-OHdG (8-hydroxy-2'deoxyguanosine). However, several of these markers suffer from artefactually generated oxidative lesions during sample preparation, especially when using archival material.

In this thesis several markers of lipid peroxidation and protein oxidation were established and applied to cell cultures and in a dietary-induced obesity mouse model. Goals were to establish HHE and HNE- (omega-3 and omega-6 derived lipid peroxidation products) protein adducts and the usage of a reporter molecule (C_{11}-bodipy) for measuring lipid peroxidation. Protein carbonyl detection via the DNPH-labelling procedure was also investigated as a marker of protein oxidation. The effects on lipid peroxidation by supplementing cell lines with different concentrations of the fatty acids palmitic acid (PA, saturated), docosahexaenoic acid (DHA, omega-3) and arachidonic acid (AA, omega-6) were studied. Also, the subcellular localization of HHE- and HNE adducts was examined. Moreover, oxidative stress in a dietary obese mouse model which received 45% of its total calories from fat compared to normal diet (10% of its total calories from fat) over six weeks was investigated.

We successfully established HNE protein adducts as a marker of lipid peroxidation both by immunocytochemistry and using slot blot analysis. Due to time limits, the development of HHE adducts procedure was not completed. HNE adduct analysis by a slot blot assay was sensitive enough to detect differences between young and adult mice and is therefore considered a suitable method to examine oxidative stress in archival tissues. The establishment of protein carbonyl measurement by using immunocyto- and histochemistry were found to have relatively poor sensitivity due to background labeling most likely from other cellular molecules. However, an ELISA-based method to measure protein carbonyls in plasma plasma and epididymal fluid was successful. The reporter assay using the C_{11}-bodipy to measure lipid peroxidation in cultured cells also showed good performance.

Our investigation showed that supplementing cultured cells with fatty acids (especially DHA) gives a protective effect from oxidative stress, possibly through acting as oxygen radical scavengers. Omega-3 and omega-6 fatty acids did not seem to give an increase in HNE and HHE protein adduct formation after cumene hydroperoxide induced lipid peroxidation in cells. Fluorescent microscope investigation of subcellular localization showed that HNE adducts are partly localized with mitochondria. Exposing mice to a high fat diet over six weeks seems to protect against the formation of HNE adducts in testis, contrary to our expectations.

Table of contents

Abbrevations

AA	Arachidonic acid
BHT	Butylated hydroxytoluene
CLPAA	Cellular lipid peroxidation antioxidant activity assay
CumOOH	Cumene hydroperoxide
DHA	Docosahexaenoic acid
DMSO	Dimethyl sulfoxide
DNP	2,4-dinitrophenyl
DNPH	2,4-dinitrophenylhydrazine
EPA	Eicosapentaenoic acid
FA	Fatty acids
FCS	Fetal calf serum
H_2O_2	Hydrogen peroxide
HHE	4-hydroxy-2-hexenal
HNE	4-hydroxynonenal
HRP	Horseradish peroxidase
KO	Knockout
LPR	Lipid peroxidation rate
PBS	Phosphate-buffered saline
PC	Protein carbonyl
PUFA	Polyunsaturated fatty acid
ROS	Reactive oxygen species
TBARS	Thiobarbituric acid reactive substances
TBS	Tris-buffered saline
WT	Wild type

1 Introduction

1.1 General background on oxidative stress and oxidative damages

All organisms are continuously being exposed to reactive oxygen species. Unbalanced reactive oxygen species are known to cause oxidative damage to cellular macromolecules, which may eventually lead to the development of diseases. Biological markers for oxidative damage are therefore important in order to detect such damages, and numerous detection methods of oxidative damage have been developed. Examples include the lipid peroxidation derived malondialdehyde and the quantification of protein carbonyls which have been extensively used.

1.1.1 Reactive oxygen species and their toxicity

Cells are continuously exposed to endogenous or exogenous sources of reactive oxygen and species (ROS), including the production of ROS by mitochondria and by ionizing radiation. Some ROS function as signaling molecules. For example, cells that are exposed to hypoxia (low concentrations of oxygen) lead to an increased mitochondrial production of ROS, including hydrogen peroxide (H_2O_2). H_2O_2 then acts as a messenger and regulates cellular responses to hypoxia (Chandel et al., 1998). However ROS may also inflict damage to cellular macromolecules (e.g. nucleic acids, proteins and lipids) by reacting with and thereby altering or destroying the macromolecule structure. This process can happen in a variety of ways, by breaking lipid chains, site-specific amino acid modification of proteins, enzyme inactivation, strand breakage and modifications of DNA to mention some examples. The hydroxyl radical ($HO^{\bullet}$) is the most potent radical and may attack cellular macromolecules by abstracting a hydrogen atom. The potential harmful effects of ROS are under normal conditions regulated by antioxidant systems in the cell.

1.1.2 Antioxidants, oxidative stress and diseases

Antioxidants are crucial for detoxifying ROS, and they are either enzymatic or non-enzymatic. The enzymatic antioxidant defense includes superoxide dismutase (SOD) that converts $O_2^{\bullet-}$ to H_2O_2 and glutathione peroxidase (GPx) and catalases which can detoxify H_2O_2. Non-enzymatic antioxidants include vitamin C and E, glutathione and melatonin, which reacts directly with ROS and thereby detoxifies them. If the concentrations of ROS overwhelm the antioxidant defense systems in a cell, this imbalance is called oxidative stress (Halliwell, 2007). This condition can occur due to an increase in ROS or as a decrease in the cellular defense, or a combination of the two. ROS may also initiate oxidation of lipids, a process called lipid peroxidation. If this process is not stopped, more ROS are produced as well as other reactive molecules (e.g. reactive aldehydes) which ultimately cause more oxidative damage to cellular macromolecules. Many types of oxidative damages are continuously repaired, but oxidative damages are still thought to be a major cause of cellular functional decline and aging (Hayflick, 2007).

Oxidative stress is related to a number of medical conditions (figure 1.1) including obesity,

cancer and neurodegenerative diseases such as Alzheimer's and Parkinson's (Beal, 2002). A variety of stressors, including chemical exposures and nutritional stress, have been shown to induce oxidative stress; to explore the role of oxidative stress in toxicity and disease development robust markers are required.

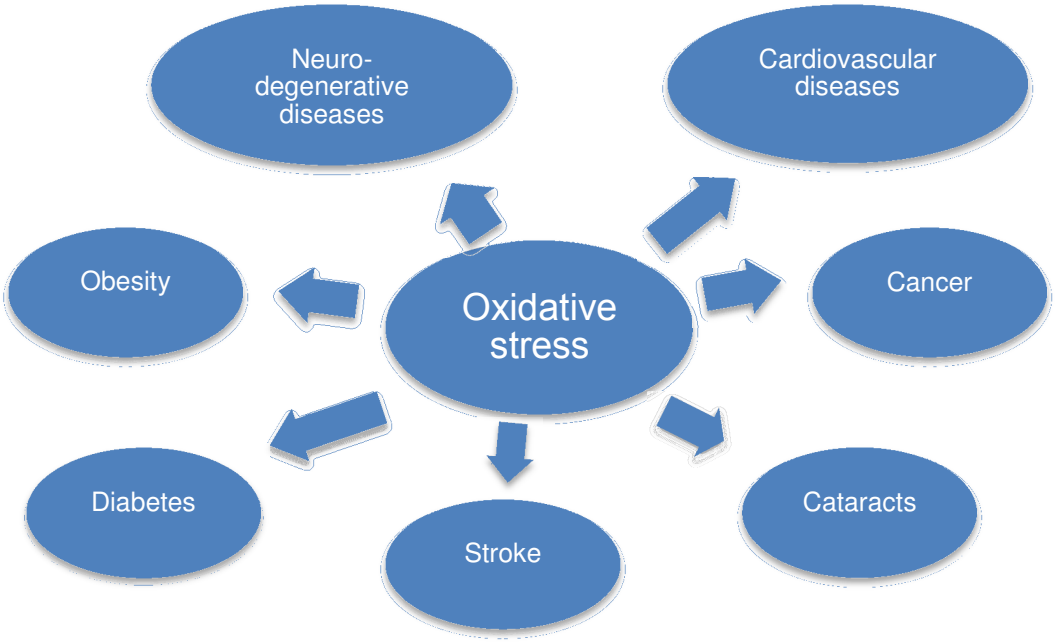

Figure 1.1 Conditions related to oxidative stress

1.2 Biological markers of oxidative stress

A biological marker may be defined in various ways, and has been defined by the National Institutes of Health (NIH) working group as "A characteristic that is objectively measured and evaluated as an indicator of normal biological processes, pathogenic processes, or pharmacological responses to therapeutic intervention." (Atkinson A.J. et al., 2001). An ideal biological marker is specific, predictive, sensitive, accessible and robust. ROS have extremely short half-lives and are difficult to measure, and is therefore generally not suitable as biological markers (Kohen & Nyska, 2002). Many different biological markers of oxidative stress have been developed over the last years regarding oxidation of lipids, proteins and DNA, and some of them are shown in table 1.1. Examples include thiobarbituric acid reactive substances (TBARS) assay which measures malondialdehyde (MDA, a lipid peroxidation end-product), protein carbonyls (oxidative damage to proteins) and 8-hydroxy-2'–deoxyguanosine (8-OHdG) (DNA damage). However, there are weaknesses concerning many of these markers. For example, the TBARS assay measures MDA, but as there are other sources of MDA than lipid peroxidation the test is not specific (Del Rio et al., 2005). This assay also involves boiling the tissue and therefore potentially introduces false positives. 8-OHdG as a marker for DNA oxidation also has disadvantages. DNA is

susceptible to oxidation, and laboratory techniques tends to induce oxidation of DNA by ambient oxygen concentrations and transition metal ions which potentially causes false positives when applying 8-OHdG as a marker (Valavanidis et al., 2009).

Biomarker	Advantages	Disadvantages
Isoprostanes (IsoPs)	Can be detected in various samples (serum, urine).	Current methods of quantification are impractical for large-scale screening (GC/MS) or require further validation (immunoassay kits).
Malondiealdehyde (MDA)	Technically easy to quantify spectrophotometrically using the TBARS assay. ELISA kits to detect MDA also have good performance.	TBARS assay is non-specific and sample preparation can influence results.
ROS-induced changers to gene expression	The expression of several genes may be measured simultaneously using microarray technology.	Microarray technology can be manually and computationally expensive.
Serum antioxidant capacity	Commercial kits available to measure antioxidant capacity. Can be utilized on frozen samples.	Antioxidant activity in serum may not reflect microdomains important to the pathogenesis of relevance.
Protein carbonyls	Chemically stable and therefore easily detected. ELISA kits are available.	Protein carbonyls are naturally abundant, which may lead to sensitivity issues
8-hydroxy-2'-deoxyguanosine (8-OHdG)	Sensitive marker of DNA damage.	Sample preparation can influence result by oxidation of DNA

Table 1.1 Biological markers of oxidative stress. *The table summarizes advantages and disadvantages of various biological markers of oxidative stress. Modified from Ho et al., (2013)*

Using modifications of proteins as biological markers may be beneficial due to the fact that proteins are quite stable, and as a result, the risk of inducing oxidative artifacts is generally low. Moreover, the abundance of proteins found in plasma, cells and tissues is generally higher than DNA, RNA and lipids. Sensitive assays that can measure under which conditions oxidative damages to proteins (i.e. protein carbonyls) and lipid peroxidation are in demand, and establishing such assays was a part of this assignment, including 4-hydroxy-2-nonenal (HNE) and 4-hydroxy-2-hexenal (HHE) as markers of lipid peroxidation and protein carbonyls as markers of protein oxidation.

1.3 Protein carbonyls

Carbonyls are a functional group consisting of a carbon atom that has a double bound to an oxygen atom. This means that aldehydes, ketones, carboxylic acids, esters and amides are all carbonyl groups. Oxidation of certain amino acids within proteins can result in formation of protein carbonyls (PCs) which are disturbers of protein function (Dalle-Donne, Rossi, et al., 2003), either by modifying their structural function or by causing loss of catalytic activity. Oxidation can arise from direct oxidation of most protein residues or with secondary oxidation products such as HNE or HHE (Beal, 2002). Protein carbonyls have been linked up

to as a marker of aging (Nyström, 2005) and it has been shown that protein carbonyl content increases drastically in the last third of the lifespan, reaching a level where averagely one out of every three protein molecules has a protein carbonyl modification (Stadtman, 1998). Protein carbonyls has also been shown to be involved in diseases such as Parkinson's and Huntington's disease (Beal, 2002). Due to their chemical stability they are also good markers of oxidative stress. Protein carbonyls can be marked with 2,4-dinitrophenylhydrazine (DNPH) which binds to carbonyls associated with aldehydes and ketones, but not with carbonyls such as esters, amides and carboxylic acids. Aldehydes and ketones are derivatized by DNPH, which leads to the formation of the stable 2,4-dinitrophenyl (DNP) hydrazone product (Alamdari et al., 2005). Antibodies have been developed to bind to DNP.

1.4 Lipids and lipid peroxidation

1.4.1 Fatty acids

The intake of polyunsaturated fatty acids (PUFAs) plays an important role for human health. For instance, the intake among children is thought to be beneficial for brain development (Uauy et al., 2001). However, under conditions of oxidative stress PUFAs are particularly vulnerable towards lipid peroxidation, a process generating multiple reactive aldehydes, forming undesirable adducts on biomolecules such as proteins and nucleic acids (Pizzimenti et al., 2013). If the adducts are not repaired it may lead to protein dysfunction and DNA mutations.

Fatty acids are molecules consisting of a carboxyl group and a long hydrocarbon chain. They may be saturated having zero double bonds in their hydrocarbon chain, or unsaturated with one (mono) or several double bonds (poly). PUFAs are important components of the cellular membrane. They are important for membrane fluidity, may act as hormone precursors, or be modified to make signaling molecules (Spector, 1999).

In cellular systems, fatty acids are almost always bound to diglyceride, a phosphate group and an organic molecule such as ethanolamine or choline, in which they are called phospholipids. Phospholipids are incorporated into all cellular membranes, where they are formed as lipid bilayers. These phospholipids may also act as signaling molecules within the membrane. For example, phosphatidylinositol is concentrated on the cytosolic side of the membrane and can be phosphorylated by various lipid kinases, such as phosphoinositide 3-kinase. Moreover, fatty acids are important as an energy source because they can be broken down through a process called β-oxidation within the mitochondrial matrix. Reactive oxygen species can initiate lipid peroxidation which generates toxic secondary species that react with cellular macromolecules. The species formed depend on the type of lipid present in cellular membranes, but polyunsaturated fatty acids (PUFAs) are often affected due to the presence of multiple double bonds. Lipid peroxidation is split into three distinct phases (only two phases are shown in figure 1.2): initiation, propagation and termination (*Catalá*, 2006). In the initiation phase a ROS abstracts a hydrogen atom from the fatty acid, creating a radical. The fatty acid radical is an unstable molecule, which may react with molecular oxygen to form a peroxyl radical. The peroxyl radical can abstract a hydrogen atom from a free fatty acid resulting in a fatty acid peroxide and a new fatty acid radical. This is a chain reaction, which

proceeds until the lipid peroxyl radical reacts with another radical, forming a non-radical. The mechanism described in figure 1.2 valid for any PUFA, including arachdonic acid (an omega-6 fatty acid) and the fish oils docosahexaenoic acid and Eicosapentaenoic (both omega-3 fatty acids acid).

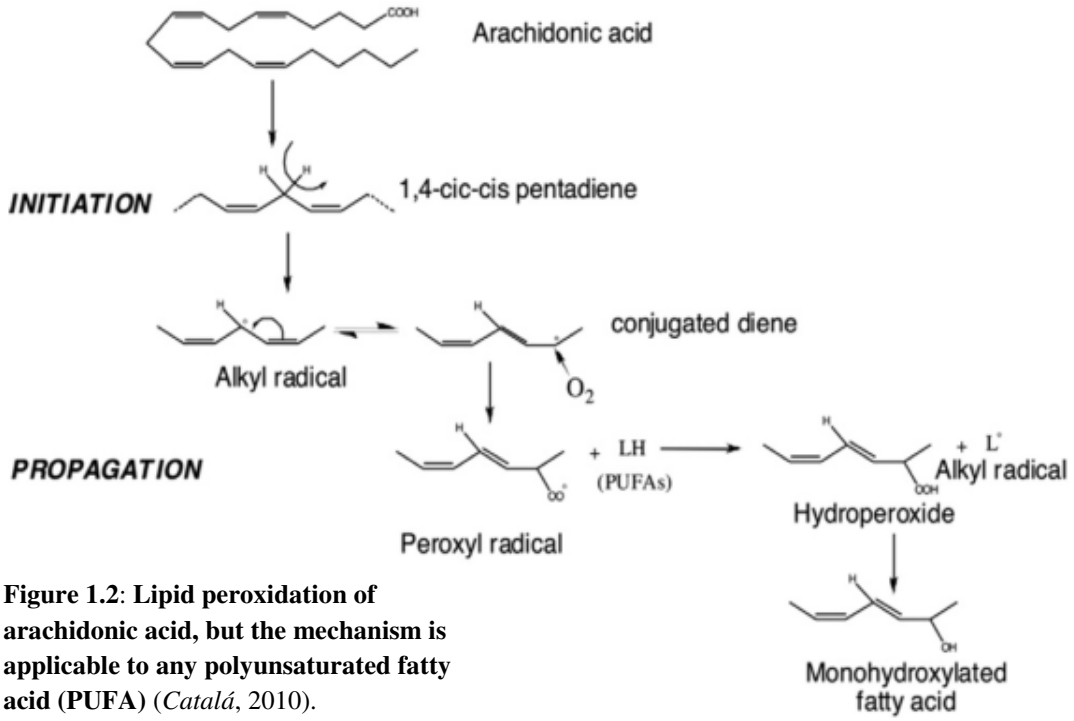

Figure 1.2: **Lipid peroxidation of arachidonic acid, but the mechanism is applicable to any polyunsaturated fatty acid (PUFA)** (*Catalá*, 2010).

The mechanism described in figure 1.2 is valid for any PUFA, including arachdonic acid (an omega-6 fatty acid) and the fish oils docosahexaenoic acid and Eicosapentaenoic (both omega-3 fatty acids acid). The lipid peroxidation of DHA and AA may lead to the formation of the products HHE (4-hydroxy-nonenal) and HNE (4-hydroxy-2-hexenal) (figure 1.3).

Docosahexaenoic acid (DHA)

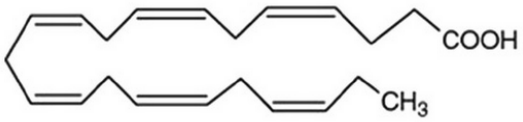

Arachidonic acid (AA)

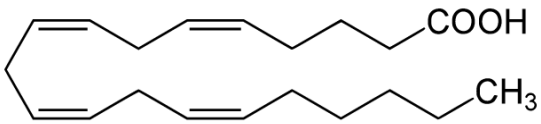

4-hydroxy-2-hexenal (HHE)

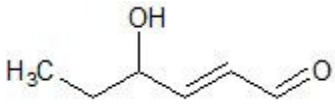

4-hydroxy-2-nonenal (HNE)

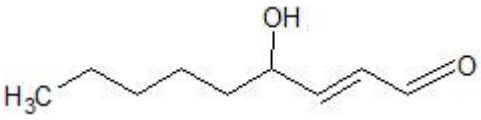

Figure 1.3 Docosahexaenoic acid (DHA) and arachidonic acid (AA) and their lipid peroxidation derived aldehydes HHE and HNE, respectively (Catalá, 2009)

1.4.2 4-hydroxynonenal and 4-hydroxy-2-hexenal (HNE and HHE)

HNE has since its discovery decades ago been studied extensively and is today considered an important biological marker for lipid peroxidation. HNE is an α,β-unsaturated aldehyde and is the main oxidation product of the omega-6 polyunsaturated fatty acids AA, and was identified as a cytotoxic product in 1980 (Benedetti et al., 1980). Over the last years a significant correlation has been shown between increased HNE content and several diseases, including neurodegenerative diseases such as Alzheimer's (Butterfield et al., 2013) and Parkinson's (Yoritaka et al., 1996), metabolic syndromes (Singh et al., 2009) and cardiovascular diseases (Vindis et al., 2006). HNEs is also involved in cancer, but studies have shown both increased and decreased levels of HNE in cancer tissue compared to healthy tissue (Marquez-Quiñones et al., 2010; Oberley et al., 1999).

HHE is also an α,β-unsaturated aldehyde and is the main oxidation product of the omega-3 polyunsaturated fatty acids DHA (Van Kuijk et al., 1990) and EPA in some tissues (Nakagawa et al., 2014). It forms adducts in the same way as HNE, but has been far less studied. Even so, elevated levels of HHE has been found in Alzheimer's disease (Bradley et al., 2012), impaired resistance to tuberculosis (Bonilla et al., 2010). Moreover, induced photooxidative retinal damage found a positive correlation between the level of the docosahexaaenoic acid, the extent of lipid peroxidation and generation of HHE, and the severity of the retinal damage (Tanito et al., 2009). HHE has also been shown to induce increased transcription rate of NF-κB (J. Y. Lee et al., 2004), which is a gene that is involved in stress-related responses. Combined, these studies show that intake of omega-3 may have

some deleterious effects that in some cases may overcome the benficial effects usually attributed to omega-3.

By increasing omega-3 and omega-6 intake, the PUFA-content of the cellular membranes also increase, at least in some organs and cell types (Baylin et al., 2002; Sun et al., 2007), thereby possibly making the cells more susceptible for lipid peroxidation and giving rise to products such as HNE and HHE.

1.5 Dietary fatty acids and obesity

There has been raised concern about the fatty acid diet in modern civilization. Humans evolved as hunters and gatherers on a diet with a ratio of omega-6 to omega-3 of approximately 1, but this has changed drastically since the agricultural revolution which started 10000 years ago. Due to this todays western diet consists of a ratio of around 15:1 (omega-6:omega-3) (Simopoulos, 2002). Omega-3 and omega-6 are involved in many of the same inflammatory pathways, a change in this ratio can therefore have important implications since omega-6 is generally known to be pro-inflammatory and omega-3 anti-inflammatory (Calder, 2009). A high omega-6:omega-3 ratio may therefore increase pro-inflammatory pathways, which may lead to inflammatory diseases such as atherosclerosis (Russel, 1999).

Obesity is an increasing problem in western societies. Approximately half of the adult population in the European Union is defined as overweight or obese. Obesity has been shown to associate with mild, chronic oxidative and inflammatory stress (Fernández-Sánchez et al., 2011) and may thus predispose to oxidative stress related diseases. It is of interest to gain more mechanistic knowledge on how obesity may predispose to disease and the importance of interactions with other stressors, like environmental pollutants.

1.6 Dietary obese mouse model

In the dietary-induced obesity model a high fatty diet is applied to induce obesity in mice. During the period of high fat diet intake, they gain weight and eventually show higher serum levels of cholesterol and free fatty acids (Bakos et al., 2011). If they maintain the high fat diet effects on intracellular ROS and mitochondrial ROS as well as DNA damage in sperm are eventually observed (Bakos et al., 2011; Duale et al., 2014). The extent of disease development and negative effects depends on the time period of high fat diet intake (Palmer et al., 2012). After three to four weeks they start gaining more weight than the group that is on a standard diet. After eight to nine weeks they develop more serious symptoms of metabolic disturbance including insulin resistance (Palmer et al., 2012).

Obese males and diet-induced animals show reduced testosterone levels and impaired sperm quality. The increased prevalence of obesity seems to correlate with a decline in in male reproductive health (Hammoud et al., 2012), and oxidative stress seems to be an important factor in this decline (Saleh & Agarwal, 2002; Tremellen, 2008).

1.7 Testis

Concerns about a potential decline in the male reproductive health have been and has been termed the testicular dysgenesis syndrome (Skakkebæk et al., 2001). Reduced sperm count, reduced sperm mobility, genital abnormalities and increased prevalence of testicular cancer have been observed during the last decades and are believed to be caused by a combination of lifestyle and environmental factors (Boisen et al., 2006). The testis has high contents of PUFAs, making it susceptible to lipid peroxidation compared to other organs (except for the brain). The primary functions of the testis are to produce sperm via spermatogenesis and to produce hormones, including testosterone. They are therefore vital for the male reproductive system.

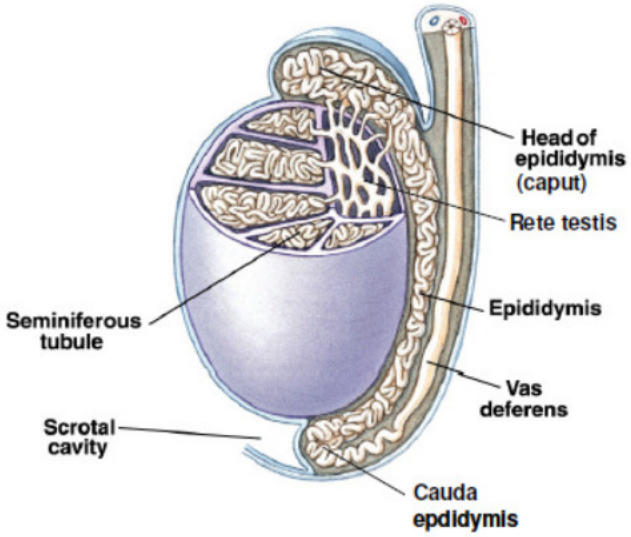

Figure 1.4: Anatomy of the human testis. *Adapted from Silverthorn et al., (2009)*

The epididymis has three functional regions, the caput, corpus and cauda. The caput epididymis is connected to the efferent ducts of the testes, and reabsorption of the fluid secreted by rete testis occurs in the caput, and the caput also secretes epididymal fluid. The maturation of sperm is a gradual process starting from seminiferous tubes and ending at the cauda, in which it is ready to fertilize eggs. Throughout this process the sperm is situated in different kinds of organic fluids. The fluids are important for several reasons, including: One being that the fluid is important to facilitate movement of the sperm after mating, another being the abundance of antioxidants in this fluid. As sperm cells consist of a high content of PUFAs they are particularly susceptible to oxidative stress and lipid peroxidation. Spermatozoa are protected by various antioxidants and antioxidant enzymes in the seminal plasma or in spermatozoa itself to prevent oxidative damage (Oxidation and the spermatozoa). Glutathione peroxidase 1 (GPX1) is present in testis, prostate, seminal vesicles, vas deferens and epididymis and is important to protect sperm from lipid peroxidation (Vernet et al., 2004). Other members of GPX are also important, including GPX5 which is found in both caput and

cauda epididymis (Rejraji et al., 2002). Furthermore, other non-enzymatic molecules such as α-tocopherol uric acid, glutathione (Halliwell, 2007) is also present in the epididymis. Following this, if ROS are abundant in the epididymis they may deplete the antioxidant capacity of the epididymal and seminal fluid and therefore make the sperm more vulnerable to oxidative stress. The presence of antioxidants is important for the protection of sperm, and it has been shown that the supplementation of antioxidants can improve the sperm quality (Yousef et al., 2003).

1.8 Aims and hypothesis

Many different stressors, including nutritional stress and environmental pollutants may induce oxygen radicals which can lead to oxidative stress if not counterbalanced by antioxidant systems. Oxidative stress may cause damage to cellular macromolecules and thereby lead to the development of a variety of diseases. Precise and robust biological markers for oxidative damage are therefore important for mapping out the exact causes of these conditions.

The general aims were to gain increased knowledge on:

- The importance of fat (amount and lipid type) consumption for people's health.
- If oxidative stress generated damages to proteins contribute to functional decline in disease.

The specific aims were to:

- ✓ Establish the CLPAA (cellular lipid peroxidation antioxidant activity) assay as an approach to study role of fatty acids on lipid peroxidation rates in cultured cells
- ✓ Establish antibody-based methods to detect stable oxidative stress protein damage markers in cultured cells and tissue:
  - Protein carbonyls
  - HNE and HHE specific protein adducts in cultured cells and archival tissue
- ✓ Apply these markers to study the effects of fatty acids and high fat diet on levels of oxidative stress in *in vitro* and *in vivo* models.

The hypotheses were:

- ❖ That supplementing PUFA (Ω-3 and Ω-6 separately) and saturated fatty acids to cultured cells would affect the lipid peroxidation (acting as accelerators or antioxidants) during induced lipid peroxidation, and that
- ❖ That supplementation with Ω-3 and Ω-6 PUFAs to cultured cells would enhance the formation of HHE and HNE protein adducts, respectively.
- ❖ That the levels of these oxidative stress markers would be higher mine on a in high fat diet (HFD) than in mice on a control diet.

2 Material and methods

Recipes for solutions and buffers can be found in A.4, and information about producers and products are listed in A.5.

2.1 Cell cultures

Ntera-2 cl.D1 (hereafter also referred to as Ntera; obtained from ATCC, USA) is a pluripotent human testicular embryonal carcinoma cell line and was used for the initial *in vitro* experiments. The cells originate from a malign carcinoma, and were obtained from a lung metastasis belonging to a 22 year old Caucasian male. The cells were grown in Dulbecco's Modified Eagle's medium (DMEM) (Lonza) with 4.5 g/L glucose, with L-glutamine and with sodium pyruvate. 10% fetal calf serum (FCS) (Lonza) along with 1% penicillin and streptomycin (Lonza) was added to the medium.

Mouse embryonic fibroblasts (MEFs) cell lines derived from mid-gestation mouse embryos from wild-type mice were utilized for most of the *in vitro* experiments. The MEF cells were a generous gift from Klungland and co-workers at the Oslo University Hospital. These cells were grown in DMEM (Lonza) with 4.5 g/L glucose, 10% FCS, L-glutamine (Lonza) and 1% penicillin and streptomycin (Lonza).

Preservation of both cell types was done by storage in liquid nitrogen, and they were cultured in 75 or 162 cm^2 flasks (Corning) at 37°C with 5% CO_2 at saturated humidity in a cell incubator. For a detailed protocol regarding cell culture management please see the appendix A.1

2.2 Preparation of fatty acids and induction of oxidative damage

2.2.1 Fatty acids

The fatty acids palmitic acid, docosahexaenoic acid and arachidonic acid all from Sigma-Aldrich, were diluted in dimethyl sulfoxide (DMSO) to 100 mM under argon gas to avoid introduction of oxygen into the tubes, which may lead to oxidation of the PUFAs. The solutions were divided into 10 and 20 µL aliquots and then immediately frozen at -80°C. They were further diluted when used in cell cultures, and never reached a DMSO concentration higher than 0.1%.

2.2.2 Induction of oxidative damage

Hydrogen peroxide (H_2O_2, Merck) was used to induce oxidation of proteins and formation of protein carbonyls. H_2O_2 can readily decompose into a hydroxyl radical via the fenton reaction

through transition metals, which may attack side chains on proteins leading to the formation of protein carbonyls (Stadtman, 1998)

Cumene hydroperoxide (CumOOH, Sigma-Aldrich) was used to induce lipid peroxidation *in vitro* and it involves hemolytic cleavage of the -O-O-bond, catalyzed by cytochrome P-450, producing the cumyloxyl radical which initiates lipid peroxidation by abstracting a hydrogen atom from the lipid (Stefek et al., 1992).

2.3 Mouse model of dietary induced obesity

2.3.1 Animals

Male mice used in this study were c57BL/bl6NTac (Taconic, USA). The mice were housed in air flow IVS racks (Innorack® IVC Mouse 3.5, Innovive) in 100% PET plastic disposable cages in a room with 12-hour light/dark cycle, and controlled humidity (55 ± 5%) and temperature (20-24°C). Water and diets were given *ad libitum*.

2.3.2 Experimental design

At the age of 5 weeks, the mice were given either a normal diet with 10% fat (SDS 10% water fuel energy (AFE) fat 824050; 10% kcal from fat, 20% kcal from proteins, 70% from carbohydrate, 4.54 kcal AFE/g), or 45% fat (SDS 45% AFE Fat 824053; 45% kcal from fat, 20% kcal from proteins, 35% from carbohydrate, 3.68 kcal AFE/g), both obtained from SDS Special Diets Services. There were four experimental groups with six individuals per group:

Group 1: Followed a normal diet and exposed to PBS (vehicle) 1 week before sacrifice
Group 2: Followed a normal diet, and exposed to 61 mg/kg bw glycidamide dissolved in PBS 1 week before sacrifice
Group 3: Followed a high fat diet, and exposed to PBS 1 week before sacrifice
Group 4: Followed a high fat diet, and was exposed to 61 mg/kg bw glycidamide dissolved in PBS one week before sacrifice

The animals were humanely sacrificed at an age of 11 weeks. The experiment was performed in conformity with the laws and regulations for animal experiments and was approwed by the National Experimental Animal Board. This was done prior to this thesis and in this assignment we focused on the effects of the high fat diet compared to a normal diet. The groups were therefore reduced from four to two, with animals on a high fat diet (group 3) and animals on a normal diet (group 1) for the purpose of this thesis, with six individuals from each group.

2.3.3 Tissue homogenization

The frozen tissue had been stored at -80°C until use. The tissue samples were fragmented using a pestle or tweezers while still wrapped with the aluminum-foils. Approximately 15 mg of tissue transferred to the pre-filled tube containing lysis solution (RIPA-buffer). In homogenization run using the Tissue Lyser II (QIAGEN) four samples at a time were homogenized using a program at 20 hz for 2 minutes. The samples were turned 180 degrees, and then ran again at 20 hz for another two minutes. After homogenization the samples were transferred to new tubes and then spun down for 20 minutes at 13.4 *g at 4°C. The supernatant was transferred to a new 1.5 mL Eppendorf tube (VWR), and 30 µL was pipetted to a 1.5 mL Eppendorf tube for protein concentration measurement. The lysates were stored at -80°C.

2.4 Cellular lipid peroxidation antioxidant activity (CLPAA) assay

ROS may lead to lipid peroxidation as explained in the introduction (section 1.4). The CLPAA assay is based on a reporter molecule (C_{11}-bodipy 581/591, Life Technologies) as a marker of lipid peroxidation. This is different from many other methods because in contrast to measuring lipid peroxidation derived products such as malondialdehyde and HNE it uses a reporter molecule. As C_{11}-bodipy is highly lipophilic, it is not found in the cytosol or in the nucleus (Drummen et al., 2002). This makes it a specific marker for lipid peroxidation.

This method indirectly measures the lipid peroxidation rate in live cells. The fluorescent probe C_{11}-bodipy dissolves into cellular membranes and upon oxidation it shifts from red to green fluorescence (Drummen et al., 2002). The green fluorescence is measured by a plate reader at 485/520 nm.

2.4.1 Test of the CLPAA Assay and procedures for induction of lipid peroxidation assay

An initial experiment was performed in which different inducers of lipid peroxidation were tested out, namely the oxidants cumOOH alone or in combination with the iron-containing substances hemin (Sigma-Aldrich) and iron sulphide (Sigma-Aldrich).

After splitting of Ntera-cells they were seeded (~80000) into a 96-well plate with transparent bottom (Corning) and were allowed to settle overnight at 37°C. Following this the cells were divided into six groups (table 2.1)

Treatment 1	Control
Treatment 2	50 µM cumOOH
Treatment 3	50 µM cumOOH + 80 nM hemin
Treatment 4	50 µM cumOOH + 400 nM hemin
Treatment 5	50 µM cumOOH + 10 µM iron sulphide
Treatment 6	50 µM cumOOH + 80 µM iron sulphide

Table 2.1: Experimental setup for the CLPAA test. The experiment was not repeated (n=1) and had 8 technical replicates.

Cells were washed once in PBS once before incubating for 1 hour with hemin or iron sulphide in treatment medium (DMEM without FCS), or only treatment medium at 37 °C. Cells were washed once in PBS and then incubated with 5 μM C_{11}-bodipy (Life Technologies) in treatment medium for 30 minutes at 37ºC. Cells were washed in PBS once before adding Hanks' saline solution without phenol red (Biochrom) containing 50 μM cumOOH or simply Hanks' for the control. The plate was immediately inserted into a plate reader and read at 485/520 from the bottom. The reading was stopped after 15 minutes and linear regression models were made for each treatment. The experiment was done once with 8 technical replicates.

2.4.2 CLPAA assay – 2 experiments with PUFAs

For the first experiment if preincubation with PUFAs could affect the cellular response to the oxidant cumOOH. For the second experiment we investigated if the PUFAs by themselves could lead to altered baseline lipid peroxidation without the presence of cumOOH, after 24 and 48 hours. The second experiment was planned for the Ntera-cells, but due to high passage numbers a new batch of cells were needed for the subsequent experiments. However, due to problems with the viability and growth of new batches of Ntera cells, we were not able to get new cells up and going. We therefore switched to MEF-cells (see chapter 2.1) for the second part.

After splitting the cells they were seeded in 96-well plates with transparent bottom. 80000 Ntera-cells were seeded out in each well for the first experiment, whereas 20000 MEF-cells were seeded out in each well for the second experiment. MEF-cells were seeded out in a lower count due to their larger size. All cells were seeded out with supplementation of fatty acids (figure 2.1) and allowed to settle and grow for 24 hours. After 24 or 48 hours of incubating with fatty acids the CLPAA assay protocol followed as described below in 2.4.3

The treatment locations in the plate were randomized for each experiment. The experiments were repeated 4 times each (n=4).

Treatment experiment 1	Treatment experiment 2 24 and 48 hours
Medium only (control)	Medium only (control)
0.1% DMSO (control)	0.1% DMSO (control)
0.1% DMSO + 50 µM cumOOH	0.1% DMSO + 50 µM cumOOH
25 µM palmitic acid + 50 µM cumOOH	25 µM palmitic acid
50 µM palmitic acid + 50 µM cumOOH	50 µM palmitic acid
100 µM palmitic acid + 50 µM cumOOH	100 µM palmitic acid
25 µM docosahexaenoic acid + 50 µM cumOOH	25 µM docosahexaenoic acid
50 µM docosahexaenoic acid + 50 µM cumOOH	50 µM docosahexaenoic acid
100 µM docosahexaenoic acid + 50 µM cumOOH	100 µM docosahexaenoic acid
25 µM arachidonic acid + 50 µM cumOOH	25 µM arachidonic acid
50 µM arachidonic acid + 50 µM cumOOH	50 µM arachidonic acid
100 µM arachidonic acid + 50 µM cumOOH	100 µM arachidonic acid

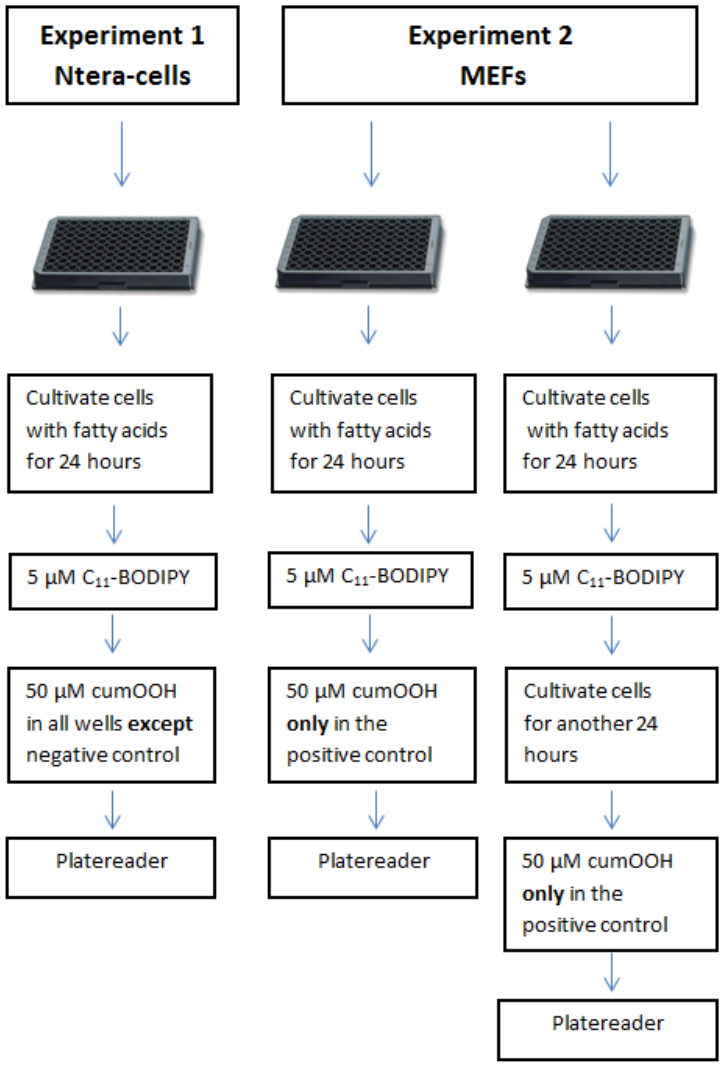

Figure 2.1: Shows the treatments and concentrations cell were exposed to, as well as the two different setups. Note that for the second experiment cumOOH was only used as a positive control in one of the treatments.

2.4.3 Assay protocol

2.4.3.1Experiment 1

After 24 hours of incubation with fatty acids the medium was removed by suction and the wells were washed with 100 µL PBS once. 5 µM C11-bodipy dissolved in 100 µL treatment medium was added to each well and incubated for 30 minutes at 37°C. All solution was removed and the cells were washed with 100 µL PBS once. 100 µL of Hanks saline solution without phenol red (Biochrom) was added to each well. For all the treatment groups in the first part, the Hanks solution contained 50 µM cumOOH, which induces lipid peroxidation. The 96-well plate was immediately after inserted into a plate reader (CLARIOstar, BMG Labtech) with a reading every three minutes for an hour. The incubator in the plate reader was set at 37°C in advance, and the monochromator was adjusted to read at 485/520 nm from the bottom. The data was analyzed, making linear regression models for each treatment. The slope was used as a marker for lipid peroxidation rate.

2.4.3.2 Experiment 2

After incubation with the various treatments for 24 hours both plates were incubated with 5 µM C11-BODIPY in 100 µL treatment medium at 37°C. One plate was left for incubation for another 30 minutes, whereas the other one was incubated for 24 hours. After incubations, the plates were washed once in PBS and then incubated with 100 µL Hanks saline solution or 100 µL Hanks saline solution containing 50 µM cumOOH for the positive control for 30 minutes at 37°C. The plates were inserted into the plate reader and read at 485/520 nm from the bottom. An endpoint measurement was applied for the second part.

2.5 Protein carbonyl detection by immunocyto and histochemistry and ELISA

Protein carbonyls are known markers of oxidative stress as described in the introduction (1.3). 2,4-Dinitrophenylhydrazine (DNPH) has for several decades been used to mark protein carbonyls. DNPH binds to carbonyls of the aldehyde and ketone type, but not with carbonyls such as esters, amides and carboxylic acids. Aldehydes and ketones are derivatized by DNPH (Dalle-Donne, Rossi, et al., 2003), which leads to the formation of 2,4-dinitrophenyl (DNP) hydrazone product. The product is stable, and an anti-DNP antibody may then be applied to label DNP. The objective was therefore to first establish methods for accurately detecting this biomarker, and then to use them *in vitro* and *in vivo* for detection of oxidative stress.

2.5.1 Protein carbonyl immunocyto- and histochemistry

Attempts were first done by exposing Ntera-cells to H_2O_2 by the following procdure: After splitting of cells, the remaining cell suspension was divided into 1.5 mL Eppendorf tubes containing different doses of H_2O_2, 50 µM, 100 µM and 500 µM plus a control containing only PBS. This was followed by incubation for 30 minutes at 37°C allowing formation of protein carbonyls. The cells were centrifuged at 400 * g for 4 minutes. The supernatant was pipetted out and an appropriate volume of PBS was added giving approximately $1.5 * 10^6$

million cells/mL. 10 µL of the cell suspension (~ 15000 cells) was added to a slide. After dehydration on a heated plate, a hydrophobic ring was drawn around all samples with a hydrophobic PAP pen (Vector Laboratories). The slides were fixated by placing them in a methacarn (methanol, chloroform and acetic acid, 60/30/10) bath for 10 minutes at room temperature. Formaldehyde was not used as a fixative since formaldehyde itself is a carbonyl and would therefore introduce artificial carbonyls. After this rehydration and antibody procedure followed.

After fixation, the cells were rinsed in deionized water before rehydration in TBS-buffer for 10 minutes. Slides were then incubated in TBS for 5 minutes 3 times. 100 µL of 10 µM DNPH-solution was added to each sample, and slides were incubated for 30 minutes at room temperature in the dark, followed by washing of slides in TBS buffer for 5 minutes 3 times. 100 µL of blocking buffer (Background punisher, Biocare Medical) was added to each sample and incubated for 10 minutes at room temperature. Slides were washed in TBS buffer 5 minutes 3 times. 100 µL of the Anti-DNP (Life Technologies) antibody was added to each sample and left to incubate overnight in dark at 4 °C degrees. This antibody is conjugated to an Alexa Fluor 488. Samples were washed in TBS buffer for 5 minutes 3 times. Slides were rinsed in distilled water and 2 drops of fluorescent mounting media were added to each sample. A cover slip was added and the slides were investigated using a fluorescence microscope (Axio Observer Z1, Zeiss).

Attempts on using the same principles for *in vivo* purposes were also done. Liver tissue from mice was used to test the method and exposed to different doses H_2O_2 and fixated in methacarn, Tissues were paraffin-embedded (Histo Comp,Vogel) by using Shandon Excelsior ES (Life Technologies). After paraffin-embedding the samples, a microtome (Microm HM 355S, Life Technologies) was used to cut 4 µM thin sections, followed by rehydration and antibody procedure (all steps described in details in A.2) and then investigated under a microscope.

2.5.2 Protein carbonyl ELISA

ELISA is an alternative method for measurement of protein carbonyl content and most suitable for samples were nucleic acid content is low and was therefore applied in plasma and epididymal fluid. The presence of carbonyls in nucleic acids may result in false positive staining.

The objective was to evaluate if a high fat diet *in vivo* could have an effect on protein carbonyl content. To investigate this we quantified protein carbonyl content in plasma samples as well as from caput epididymis and vas deferens fluid by using an ELISA kit (OxiSelect™ Protein Carbonyl ELISA Kit, Cell Biolabs) and following the procedures described in the kit. This kit determines the protein carbonyl content by measuring the absorbance of each sample and comparing it to a standard curve with known carbonyl content.

Existing plasma, and fluid isolated from caput epididymis and vas deferens were thawed.

Protein quantification was done by applying a Lowry Protein assay kit (DC Protein Assay, Bio-Rad). For samples taken from the plasma the protein samples were diluted to 20 µg/ml PBS (total 100 µL). For samples taken from the vas deferens and caput epididmys the protein samples were diluted to 10 µg/ml PBS (total 100 µL). The standard curve was prepared by mixing oxidized and reduced BSA in proper ratios in accordance with kit description giving a standard ranging from 0 to 7.5 nmol/mg protein carbonyl.

Protein samples or BSA standards were added to a well plate overnight at 4 °C, allowing adsorption of the proteins to the plate. DNPH was added that binds carbonyl groups on proteins, this allows for an anti-DNP antibody binding to the product, followed by a horse radish peroxidase (HRP) conjugated secondary antibody. Absorbance of the secondary antibody for each sample is measured and compared to the BSA standards (EL 808 Aborbance Reader, Bio-Tek)

2.6 Detection of HNE and HHE protein adducts:

HNE and HHE are known lipid peroxidation derived aldehydes after oxidation of AA and DHA, respectively. As these aldehydes are quite reactive, they may rapidly bind and form adducts to biological macromolecules such as DNA, proteins and lipids. Our main objective was to use monoclonal antibodies towards HNE and HHE protein adducts to identify these adducts *in vitro* by using immunocytochemistry and the anti HNE *in vitro* and *in vivo* for a slot blot analysis. The monoclonal antibody clone HNEJ-2 was used to mark HNE adducts. It is highly specific for HNE histidine adducts, and show little cross-reactivity with HNE lysine and cysteine residues (Toyokuni et al., 1995). For HHE adducts the monoclonal antibody , clone HHE53 was applied, which is specific for HHE histidine adducts (Yamada et al., 2004). The following protocol was based on (Majima et al., 2002), but was modified. The primary antibodies (anti-HNE and anti-HHE), secondary antibody, mitotracker and blocking-buffer concentration were adjusted in order to achieve high sensitivity and low background staining.

2.6.1 Induction of HNE and HHE adducts: detection by immunocytochemistry

After splitting of cells, 15000 cells were seeded out in 1 mL medium in chamber slides and incubated overnight at 37°C. Subsequently, the cells were incubated with either 50 µM AA or 50 µM DHA or without extra fatty acid supplementation. Medium was removed and replaced with Hanks solution containing 50 µM cumOOH (the stressor) or simply medium. This was left to incubate for 30 minutes at 37°C. Slides were rinsed in PBS buffer, followed by incubation with 500 nm of Mitotracker® Red CMH2kROS (Life Technologies) in medium for 40 minutes at 37°C to label mitochondria. Cells were fixed in 4% paraformaldehyde (Sigma-Aldrich) for 10 minutes by adding 1 mL to each chamber. Slides were rinsed in PBS buffer twice. Cells were postfixed with ethanol/acetic acid (95/5,v/v) for 2 minutes by adding 1 ml to each chamber. Slides were rinsed in PBS buffer twice. 300 µL of 1% BSA containing PBS with anti HNE monoclonal antibody (1:100, HNEJ-2, JaICA) or anti HHE monoclonal antibody (1:100,HHE53,JaICA) was added and incubated overnight in darkness at 4°C degrees. Slides were rinsed twice for 5 minutes with PBS, and then rinsed in PBS once before adding 300 µL of 1% BSA containing PBS with the secondary antibody (1:1000, 488-labelled

donkey anti-mouse IgG, Life Technologies) and incubated for 30 minutes at room temperature in the dark.

Slides were rinsed twice in PBS for 10 minutes. 300 µL of 1 µg/ml Hoechst 33342 (in PBS), to label DNA, was added to each slide and incubated for 5 minutes at room temperature in the dark. Slides were washed twice in PBS for 5 minutes, and then rinsed once in distilled water before adding fluorescent mounting media (S3023 Mounting Medium, Dako).

2.6.2 HNE adduct detection by slot blot analysis

The slot blot analysis is a simple method for detection of HNE adducts in plasma and tissue. It is quite similar to western blot, but proteins are not separated based on size in a gel electrophoresis. Adjusted protein samples are loaded onto a nitrocellulose membrane and followed by a blocking step and then an incubation of the primary antibody. After this, the membrane is incubated with a horseradish peroxidase conjugated secondary antibody before incubation with a HRP substrate which allows signal amplification.

The final protocol used was modified from that in Jørgensen *et al.*, (2014). Different blocking buffer concentration and incubation time, as well as different protein and primary antibody concentrations was tested out in establishing this method. Directly pipetting samples versus using vacuum-assisted filtration was also tested out. A final protocol is presented in the next chapter.

2.6.2.1Slot blot protocol

Protein concentrations in samples were measured using a Lowry protein assay (DC Protein Assay, Bio-Rad). For cellular lysates the protein concentration was adjusted to 0.05 µg/µL, and for *in vivo* lysates it was adjusted to 0.2 µg/µL. The membrane was pre-vetted in distilled water and assembled in the 72-well Bio-dot apparatus (Schleicher & Schull). 100 µL of each sample or standard was loaded to the nitrocellulose membrane and drained by vacuum-assisted filtration. Every following incubation or washing step was done on an orbital shaker. The membrane was removed from the apparatus and blocked in 2 % non-fat dry milk in PBS for 30 minutes at room temperature. The membrane was rinsed in PBS and then incubated overnight with mouse monoclonal antibody (HNEJ-53) directed against HNE-histidine epitope diluted 1:500 at 4°C. The membrane was washed in PBS 4 x 5 minutes, and then incubated with horseradish peroxidase conjugated secondary antibody 1:2000 for 90 minutes at room temperature followed by a second washing of 4 x 5 minutes in PBS. Immune complexes were visualized by Supersignal West Dura extended duration substrate (Life Technologies) and scanned in Chemidoc™ XRS+ (Bio-Rad) for signal detection.

Band intensity values were obtained using the software Image Lab 3.0.1 (Bio-RAD).

2.6.2.2 Standard curve and establishment of method

The standard curve was based on using a 1 µg/µL HNE-BSA (HNE-BSA Control, Cell Biolabs) in PBS. 5 µL of this solution was mixed with 9.5 µL 10 µg/uL BSA in PBS plus 485.5 µL PBS, giving a total amount of 500 µL solution containing 95 µg BSA and 5 µg HNE-BSA (5% HNE-BSA), meaning that 5% of the total BSA was HNE-modified BSA. A

standard curve was based on this and was further diluted in PBS containing 0.05 µg/µL BSA to obtain the standard curve (table 2.2).

Standard	HNE-BSA (µg/mL)
1	5
2	2.5
3	1.25
4	0.625
5	0.3125

Table 2.2: HNE-BSA standard curve. *A standard curve ranging from 5 µg/mL HNE-BSA (of total BSA) to 0.3125 µg/mL HNE-BSA*

For establishment of method we wanted to first test the method out on *in vivo* material in which we expected a dose-response relationship. Based on literature research it is known that HNE adduct content increase in older individuals: We therefore took brain- and testis samples from young (2-3 months) and adult (24-27 months) mice from a previously performed study. Due to limitations on sufficient sample sizes, we included mice that had a knockout at the 8-oxoguanine glycosylase gene which encodes for a DNA repair enzyme and will not be mentioned further. Four groups with three individuals for each group (n=3) with total sample size of 12 (n=12) was therefore the setup and is summarized in table 2.3

Age	Genotype	Number of animals
Young	WT	3
	KO	3
Adult	WT	3
	KO	3

Table 2.3: Number of animals per treatment group. *Total number of mice in the experimental design was 12, and the sample size was 12 for both testis and brain.*

Samples were homogenized according to the protocol in 2.2.3 and stored at -80°C until analysis.

2.6.2.3 HNE slot blot on MEF-cells and in testis tissue from the obese mouse model
Mouse embryonic fibroblast (MEF)-cells were used in the slot blot analysis. After reaching confluence (~80%), the cells were split and followed by seeding out 500000 cells to 10 mm cell culturing dishes. The following setup was applied:

Dish 1	Control
Dish 2	Control + cumOOH
Dish 3	50 µM arachidonic acid + cumOOH
Dish 4	75 µM arachidonic acid + cumOOH
Dish 5	100 µM arachidonic acid + cumOOH

Table 2.4: Experimental setup for the slot blot analysis. The experiment was repeated three times (n=3).

After seeding out cells in the cell culturing dishes they were allowed to settle and grow for 24 hours. Medium was withdrawn from the dishes and washed with PBS once. 8 mL with Hanks' solution without phenol red containing 50 µM cumOOH was added to all dishes except the control dish, which only received PBS. After 30 minutes of incubation the cells were washed with PBS once, and then the dishes were immediately placed one an ice cold metal plate. 600 µL of PBS containing a protease inhibitor (cOmplete, Mini, EDTA-free, Roche) was added to the dishes, followed by scraping of cells and then pipetting the suspension to 1.5 mL Eppendorf tubes. Cells were lysated by a cycle of freezing the cells in liquid nitrogen and then thawing them in a water bath at 37°C. This was done four times. Following this the samples were centrifuged at 16000 * g for ten minutes, and the supernatant was transferred to a new 1.5 mL Eppendorf tube, frozen in liquid nitrogen and then stored at -80 °C degrees.

A HNE slot blot analysis was also applied on testis protein lysates from the dietary obese mice model (The mice model is described in 2.2). Due limited availability and followingly very low concentration in some of the samples the sample size was reduced from 12 to 8, with 4samples from the ND-group and 4 samples from the HFD-group. The protein lysates were thawed and the slot blot protocol followed.

2.7 Fluorescence measurements and pictures

All pictures were taken by the Axio Observer Z1 microscope (Zeiss). When taking pictures from an experiment the same exposure time was applied for every picture, so that pictures could be compared. When processing the pictures it was set a cutoff value based on the immunochemical controls, a control without primary antibody (but with secondary antibody), and a control without secondary antibody (but with primary antibody). For example, if either of the controls showed fluorescence intensity up to 700 of the tissue, 700 was set as a cutoff.

For Hoechst 33342 (staining of nuclear DNA) and mitotracker (staining of mitochondria), exposure time was adjusted for each picture take, and a cutoff value was based on non-specific staining and auto fluorescence. 300 and 400 were set as cutoff values for Hoechst 33342 and mitotracker, respectively. All immunocyto- and histochemical controls are found in appendix A.3

The fluorescence intensity measurement on protein carbonyls were obtained by circling in five random cells and measure the mean intensity of each circle. This was done on four pictures for each treatment, giving a total of 20 mean intensities for each treatment.

All pictures were analyzed by the software ZEN 2011.

2.8 Statistics

All boxplots shown in this thesis the band inside the box represents the median, the bottom and top box are the first and third quartiles, respectively. Dots are outliers outside the interquartile range. The interquartile range is defined as the difference between the third and the first quartile. The whiskers extend to the most extreme data point unless it exceeds over 1.5 times the interquartile range.

All statistical analysis was done in R 3.0.2 and p-values below 0.05 were accepted as statistically significant.

Homogeneity of variance among the residuals between the different groups were controlled by plotting the residuals of the model and a normal distribution was checked by plotting a Q-Q plot, which plots the quantile data from the model against theoretical quantiles that are normal distributed. Linearity between the two quantiles suggests normal distribution. Log- or square root transforming was applied if the data was not normal distributed or if there was significant heterogeneity of variance in order to achieve normal distribution and homogeneity of variance. If data was normally distributed Bartlett's test was applied to check for homogeneity of variance. If data was not normally distributed a Levene test was performed to check for homogeneity of variance. The package car in R was used to apply the Levene test.

For the CLPAA assay a generalized linear mixed model was applied, setting the treatments as a fixed factor, whereas the experiment day was set as random factor in order to minimize the effect of the variation seen between different runs. The package nlme in R was used.

For the protein carbonyl content in plasma a one-way ANOVA was performed. For caput epididmys and vas deferens, a Kruskal-Wallis test was performed to compare the difference between the groups. Differences between HNE adduct leveles was performed with a one-way ANOVA

For the slot blot analysis regarding differences between young and old individuals a two-way

ANOVA was performed for both testis and brain. If there were significant differences, it was followed up by a post-hoc TukeyHSD test.

3 Results

3.1 Establishment of detection methology

The methods to be used had not been applied in the MIKS laboratory before. This includes the protein carbonyl detection, the HNE and HHE detection and the cellular lipid peroxidation antioxidant (CLPAA) assay. They therefore had to be established and optimized first. The first chapter focuses on the establishment, before showing the results of oxidative stress relevant experiments in 3.2.

3.1.1 Cellular lipid peroxidation antioxidant activity (CLPAA) assay

In this first experiment we wanted to test out different inducers of lipid peroxidation, namely the oxidants cumOOH alone or in combination with the iron-containing substances hemin and iron sulphide.

After splitting of Ntera-cells they were seeded into a 96-well plate and were allowed to settle overnight at 37°C. Cells were incubated for 1 hour with hemin or iron sulphide in treatment medium at 37 °C, or just treatment medium followed by a wash in PBS before adding Hanks' containing 50 µM cumOOH or simply Hanks' for the control. The plate was immediately inserted into a plate reader and read at 485/520 from the bottom. The reading was stopped after 15 minutes and linear regression models were made for each treatment.

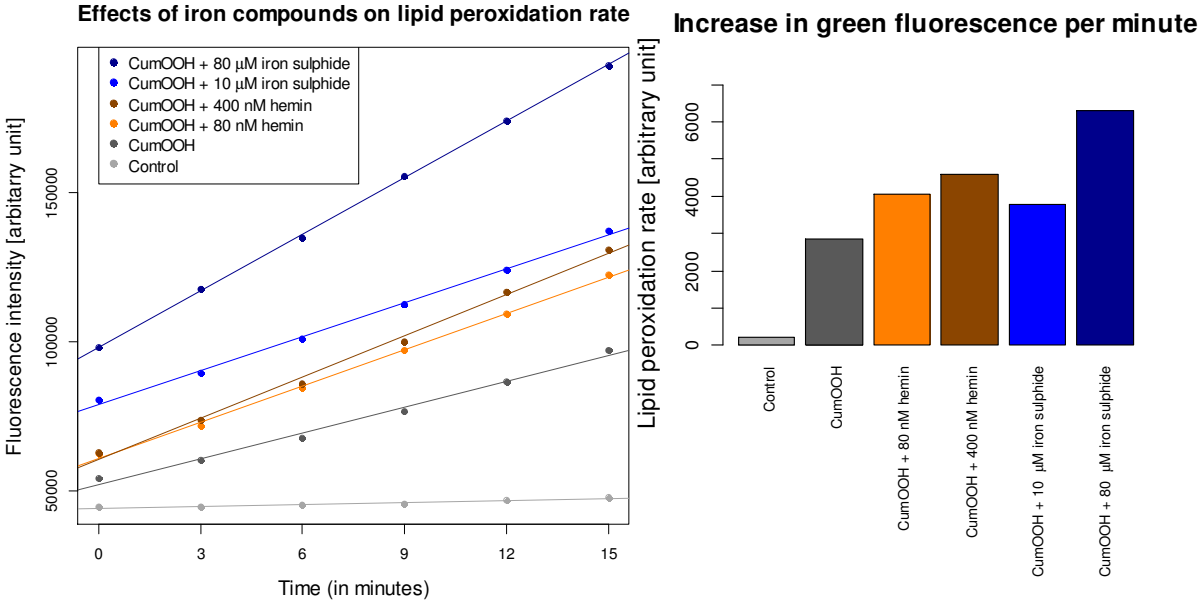

Figure 3.1: Lipid peroxidation rates after various treatments. *Cells were treated with either 50 µM cumOOH, 50 µM cumOOH + 80 nM hemin, 50 µM cumOOH + 400 nM hemin, 50 µM cumOOH + 10 µM iron sulphide , 50 µM cumOOH +80 µM iron sulphide or nothing (control). The graph on the left side shows linear regression models for the six different treatments. Amount of green fluorescence is on the y-axis and time is on the x-axis. The barplot on the right side shows the slope for each treatment. This experiment was done once (n=1) with 8 technical replicates.*

There were apparent differences between the treatments shown in figure 3.1 (left). CumOOH + 80 µM Iron sulphide giving the highest lipid peroxidation rate (LPR). The barplot in figure 3.1 (right) shows that cumOOH + 400 nM hemin gave a higher LPR than cumOOH + 10 µM iron sulphide, indicating that hemin is a more potent stressor than iron sulphide. This experiment was only done once, so no statistics were applied. We concluded that we did not need additional stressors than cumOOH for the CLPAA assay, which we would later on use as an inducer to investigate the effects of fatty acids on lipid peroxidation.

3.1.2 Protein carbonyl detection: Immunocyto- and histochemistry

In this part we attempted to establish protein carbonyls as a marker of oxidative stress. The goal was to establish the procedure in cultured cells and subsequently in liver sections.

After splitting of Ntera-cells the cells received 4 different treatments and were incubated for 30 minutes at 37°C: Control, 50 µM H_2O_2, 100 µM H_2O_2 and 500 µM H_2O_2. After treatment approximately 15000 cells were seeded out to four different slides. Fixation and antibody procedure followed until cells were investigated under the microscope.

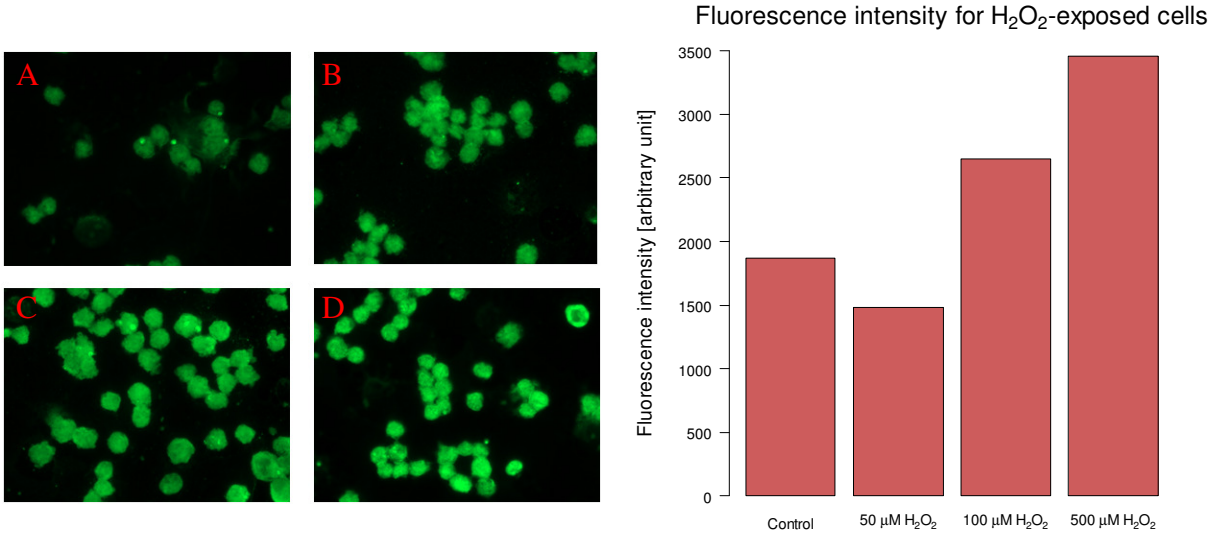

Figure 3.2: **Protein carbonyls in H_2O_2-exposed cells.** After *treatment of H_2O_2 (50 µM, 100 µM and 500 µM) and a control, cells were incubated with 10 µM DNPH followed by labeling with Anti-DNP Alexa Fluor 488. A) Control B) Exposed with 50 µM H_2O_2. C) Exposed with 100 µM H_2O_2. D) Exposed with 500 µM H_2O_2. The pictures were taken with a 40x objective. The barplot shows the mean fluorescence intensity values for the H_2O_2-treatments.*

The pictures (Figure 3.2, left) shows that the location of protein carbonyls is uniformly distributed in the cells.We can also see that the fluorescence intensity increases with the H_2O_2-exposure. This is also shown by the barplot in figure 3.2 (right). However, The lowest dose of H_2O_2 gives a slightly lower fluorescence than the control, and the highest dose displays an increase in fluorescence compared to second highest dose. The barplot was based on 4 different pictures from each treatment, and picking out 5 random cells from each picture

(pseudoreplicates=20). No statistics has been done on this since this is only taken from a single experiment. The background staining in the control limits the sensitivity assay at lower H_2O_2 concentrations.

Attempts of establishing this method was also done on *in vivo* samples, and is shown in figure 3.3. Liver tissue from a sacrificed mouse was divided into 4 equal parts followed by incubation with 2 different concentrations of H_2O_2 (5 mM and 10 mM) in PBS plus a control containing only PBS at 37°C at room temperature for 30 minutes. An immunohistochemical procedure followed before investigation under microscope.

There seems to grain-like structures in pictures B, C and D. However, the fluorescence intensity does not reflect the various treatments of these grain-like structures. The control (figure 3.3A) was exposed for a longer period compared to the pictures and therefore shows higher background fluorescence, but does not display the grains.

Several attempts of changing antibody and DNPH-concentration and blocking buffer concentration were made both *in vitro* and *in vivo*. However, we were not able to improve the sensitivty of the method and we therefore decided to move on using an ELISA-kit for detecting protein carbonyls *in vivo*.

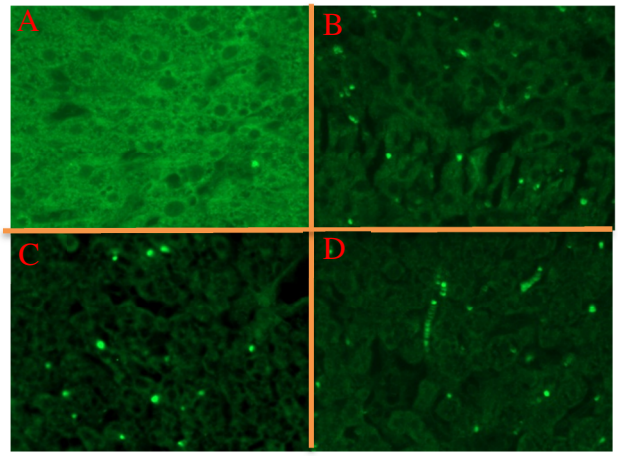

Figure 3.3: **Pictures showing two controls and H_2O_2-exposed liver tissue and stained with Anti-DNP Alexa Fluor 488.** *A control without primary antibody, B) control with antibody (not exposed to H_2O_2), C) exposed to 5 mM H_2O_2, D) exposed to 10 mM H_2O_2. The pictures show no real clear trends, and the control without antibody show autofluorescence. The control (A) was taken with a longer exposure time and therefore shows increased background fluorescence.*

3.1.3 HNE detection

In this part we wanted to establish HNE detection in a slot blot assay.

A standard curve was made (figure 3.3) with concentrations ranging from 0.3125 µg/mL to 5 µg/mL HNE-BSA. The standard curve shows clear linearity with concentrations ranging from the lowest to the highest concentration (R^2=0.996). The standard curve was made to display a linear relationship and limits of detection and not to calculate exact values.

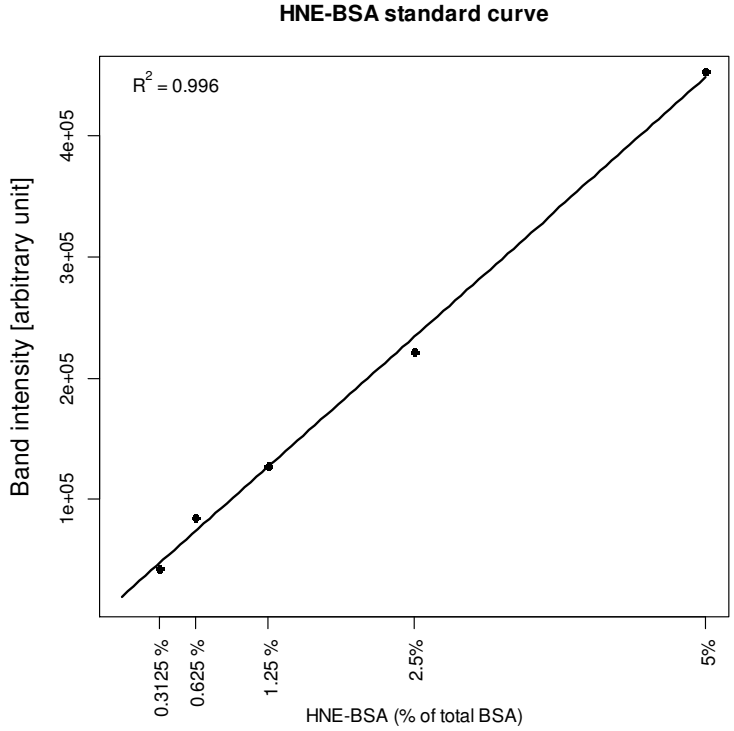

Figure 3.4: HNE-BSA standard curve. The band intensity is on the y-axis, and the concentrations are shown as % HNE-BSA of total BSA. It displays a linear relationship between band intensity and concentrations.

Furthermore, we wanted to see if this method was applicable in *in vivo* tissue. Based on literature search, markers of oxidative stress are expected to increase in older individuals in testis and brain. Existing material that had been stored at -80°C from an aging project with wild-type and transgenic (ogg knockout) mice were therefore applied. Individuals were divided into two age classes, young (2-3 months) and old (24-27 groups), and two models (WT and KO). For each group tissue lysates from three individuals were used (n=3) with a total sample size of 12 (n=12).

Controls without secondary antibody in order to exclude endogenous peroxidase were also included in this test, it is not shown in the figure but can be found in the appendix A.3.2.

For both testis and brain, there seemed to be an increase in HNE adducts in brain and testis (3.5). For the testis the age and the interaction between age and the mice model was significant (p=0.04) and gave the best model for explaining the observed data. The mice model in itself however (p=0.23, two-way ANOVA), was not an explaining factor. Both adult

WT and adult KO was significantly different versus the young WT and KO ($p<0.01$, Post-hoc Tukey's test). For the brain adult individuals seems to be different compared to young individuals, but due to large variation this is not statistically significant ($p=0.08$, two-way ANOVA), but it seems that the trend is according to what was seen in testis. The interaction between age and model was not statistically significant ($p=0.18$), and the model was not statistically significant either ($p=0.36$).

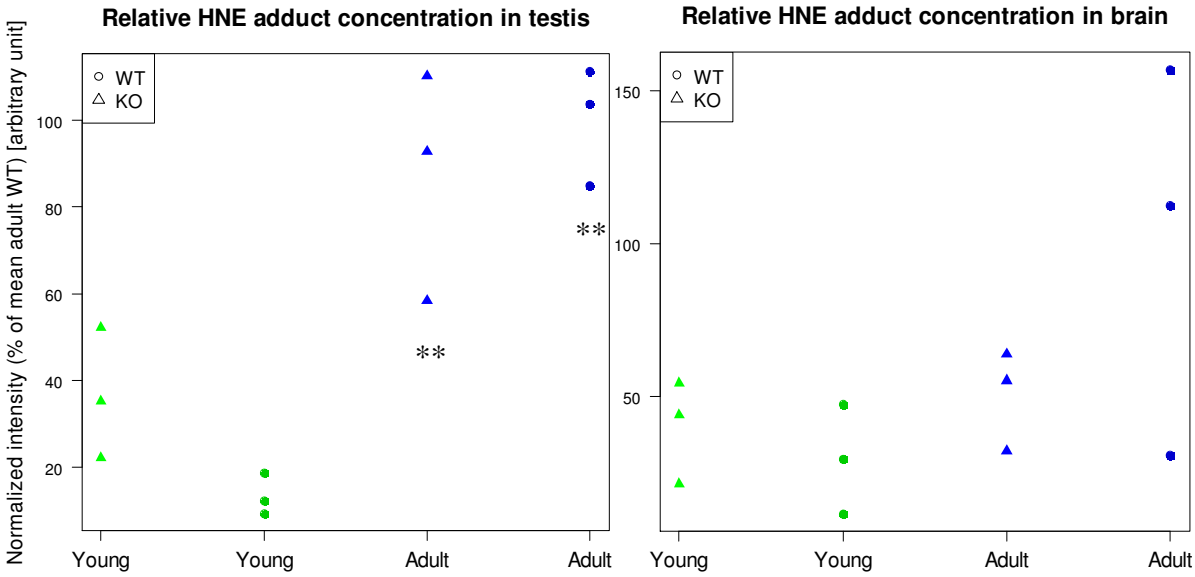

Figure 3.5: slot-blot analysis for both young (2-3 months) and adult (24-27 months) mice for KO and WT in testis (left) and brain (right). *There were three individuals per group (n=3) with zero technical replicates. **p < 0.01 statistically significant vs young WT and young KO.*

3.2 Levels of oxidized proteins in fatty acid-exposed cells and in obese mice

3.2.1 Oxidative stress in cultured cells and the effects of different types of fatty acids

3.2.1.1Effects of fatty acids on lipid peroxidation in cultured cells

The objective for this experiment was to see if fatty acids had effects on lipid peroxidation rates (LPR) by using the CLPAA assay. The effects of preincubation with different fatty acids on the susceptibility of the cells to cumOOH-induced lipid peroxidation was measured. Cells were treated with different concentrations of palmitic acid (saturated), docosahexaenoic acid (omega-3) and arachidonic acid (omega-6) in a 96-well plate and incubated for 24 hours. Following this, cells were incubated with c_{11}-bodipy for 30 minutes, treated with cumOOH and the plate was then immediately inserted into a plate reader and read at 485/520 from the bottom.

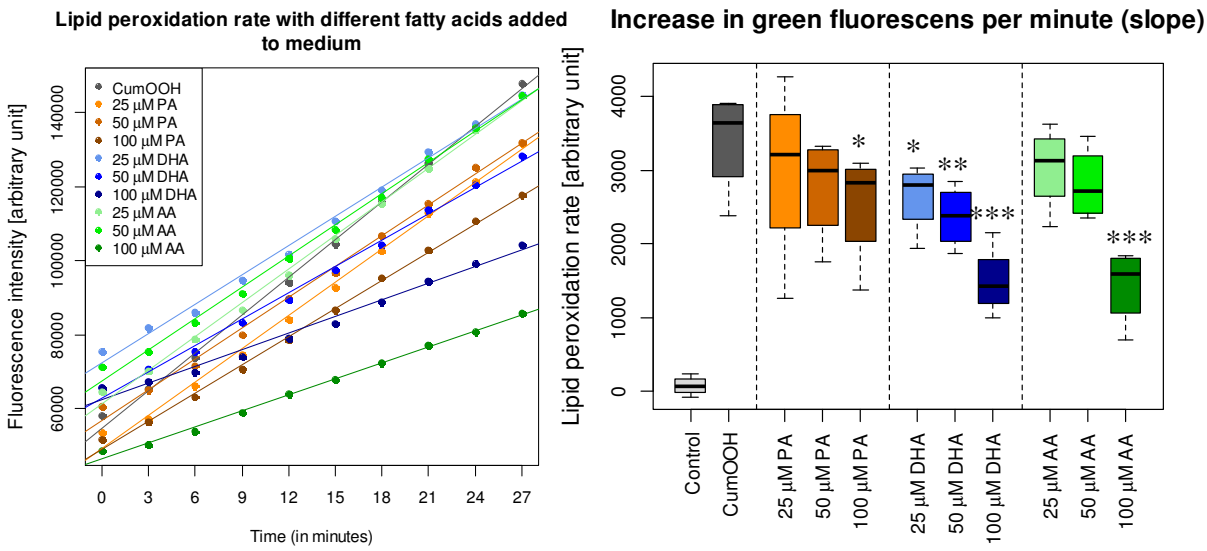

Figure 3.6*:* **Lipid peroxidation of Ntera-cells after 24 hours incubation with fatty acids.** *After incubation with fatty acids, the Ntera-cells were incubated with c_{11}-bodipy for 30 minutes, cumOOH for 30 minutes and lipid peroxidation rates was measured by fluorescence every three minutes until some measurements reached maximum fluorescence intensities (30 minutes). The graphs on the left side show linear regression models for nine different treatments. Amount of green fluorescence is on the y-axis and time is on the x-axis. Every treatment had cumOOH added (except for the control), and the cumOOH control did not have any fatty acids added to the medium. The boxplots on the right side shows increase in green fluorescence per minute. The control without cumOOH is not shown in the graphs, but is shown in the boxplots. The experiment was repeated 4 times (n=4). *p < 0.05, **p < 0.01, ***p < 0.001: Statistically significant versus CumOOH.*

The fatty acid treatments had a clear influence on LPR in response to cumOOH exposure. The LPR was highest in the cells not treated with any fatty acids (but with cumOOH), and lowest in 50 µM DHA- treatment.

Both DHA and AA treated cells significantly reduces the oxidation of the probe at all concentrations for omega-3 ($p<0.05$, $p<0.01$, $p<0.001$ for 25, 50 and 100 µM, respectively, one-way ANOVA) and at 100 µM for omega-6 ($p<0.001$, one-way ANOVA). The highest concentration of palmitic acid was also statistically significant different compared to the cumOOH ($p<0.05$, one-way ANOVA). Since we are measuring the oxidation of the probe and not the fatty acids themselves, it may be that the PUFAs were oxidized and thus acting as scavengers.

Although the cells treated without fatty acids (cumOOH) had the highest LPR, the value for green fluorescence at time zero was one of the lowest (figure 3.6) suggesting that incubation with PUFAs may introduce a low level of oxidative stress. This was further explored in the next part.

For the second part of the experiment cumOOH was only used as a positive control (figure 3.7). The cells were into two separated plates, and incubated with the fatty acids for 24 hours,

followed by 30 minutes of incubation with C_{11}-bodpy. One of the plates was left for another 24 hours of incubation. Both plates were incubated with 50 µM cumOOH for the positive control, and simply Hanks' saline solution for the other groups before reading at 485/520 from the bottom.

The 25 µM AA-treatment of cells were statistically significant versus control ($p<0.05$, one-way ANOVA). The trend seems to be that the fatty acids compared to the control show higher intensities after both 24 and 48 hours.

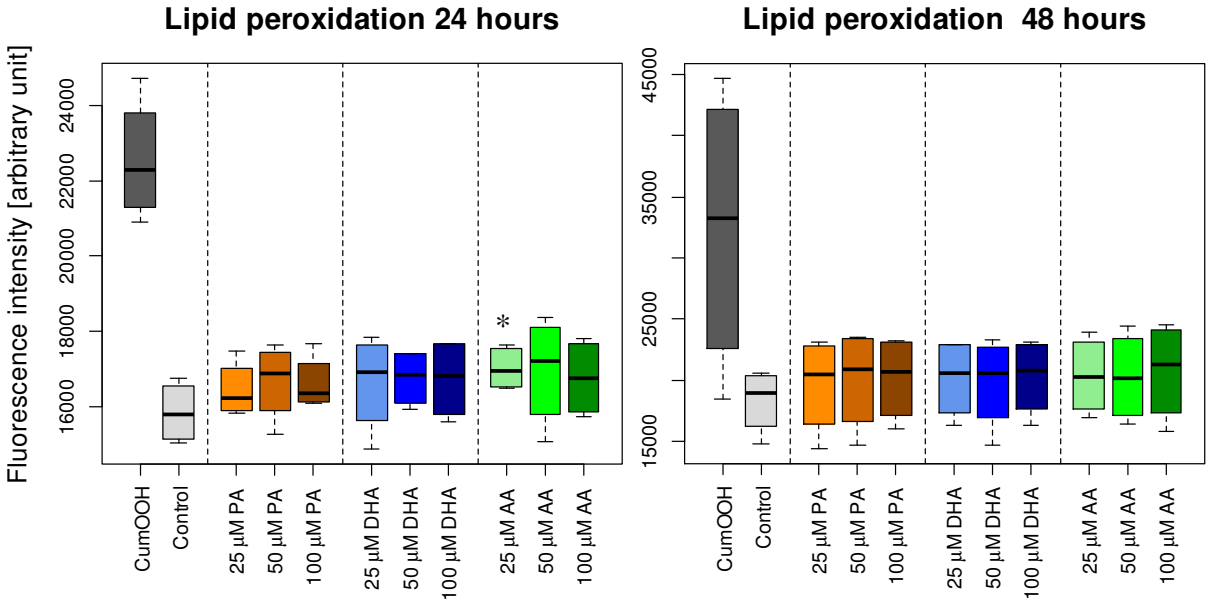

Figure 3.7: **Lipid peroxidation with an endpoint measurement after 24 hours (left) and 48 hours (right).** *Cells were incubated with fatty acids for 24 hours, and then either incubated with C_{11}-bodipy for 30 minutes or 24 hours, and then incubated with cumOOH for the positive control. Amount of green fluorescence as percentage of the positive control is on the y-axis, and the different treatments on the x-axis. CumOOH is the positive control. Both experiments were repeated 4 times (n=4) with six technical replicates.*
**p < 0.05: Statistically significant versus control.*

3.2.1.2: HNE and HHE adducts by immunocytochemistry

HNE and HHE are both known adducts that form under lipid peroxidation of Ω-6 and Ω-3, respectively. The aim was to investigate the localization of HNE and HHE adducts, and this was done by labeling the nucleus with a Hoechst dye and mitochondria with a mitotracker dye.

HNE adducts:

In figure 3.8 displays that treating the cells with cumOOH gives an increase in fluorescence intensity. Treating with cumOOH and hemin seemed to give an higher induction of HNE adducts. Incubation with 50 µM aracidonic acid (AA) did not seem to give an increase in fluorescense intensity based on the immunocytochemistry (figure 3.8) compared to the

control. However, by also treating the cells with cumOOH it seems to be a difference compared to the cells only treated with cumOOH.

The HNE adducts are located throughout the cells, but to a higher degree outside the nucleus. The anti HNE staining seems to overlap somwhat with the mitochondria. Yellow color (mix of red and green) in the overlap photos (figure 3.8 5D) indicates colocalization, meaning that the HNE adducts are in and around the mitochondria. In picture 5a, 5c and 5d (marked with an arrow) it is observed that the HNE adducts are located within the mitochondria. The adducts are also found outside the mitochondria, and there are also mitochondria unaffected by the HNE adducts.

The staining process was done several times and it was difficult to assess the results in figure 3.8 due to large variation between cells that received the same treatment making quantification of adduct levels in each treatment demanding.

HHE adducts

The HHE-staining was not fully esablished, this was due to time pressure so the results shown are prelimenary, and the staining is based on 2 experiments.

The HHE staining does not give a staining in a dose-dependant manner (figure 3.9). The control (1) shows background staining, and the cumOOH (2) does not seem to affect the HHE adduct levels. However, in the hemin-treated cells (3) the fluorescence intensity values exceeded the quantification limit and the cells seems to have rounded up. Although the majority of the cells resulted in extremely high values and rounding up, some of the cells were observed to merely affected, displaying quite low intensity values and normal cellular shape (not shown). DHA (4) in itself did not induce any effects, and might even seem to protect the cells, as only a few weak green dots are present. The DHA + cumOOH-treated cells (5) gives similar result as the cumOOH-treated cells.

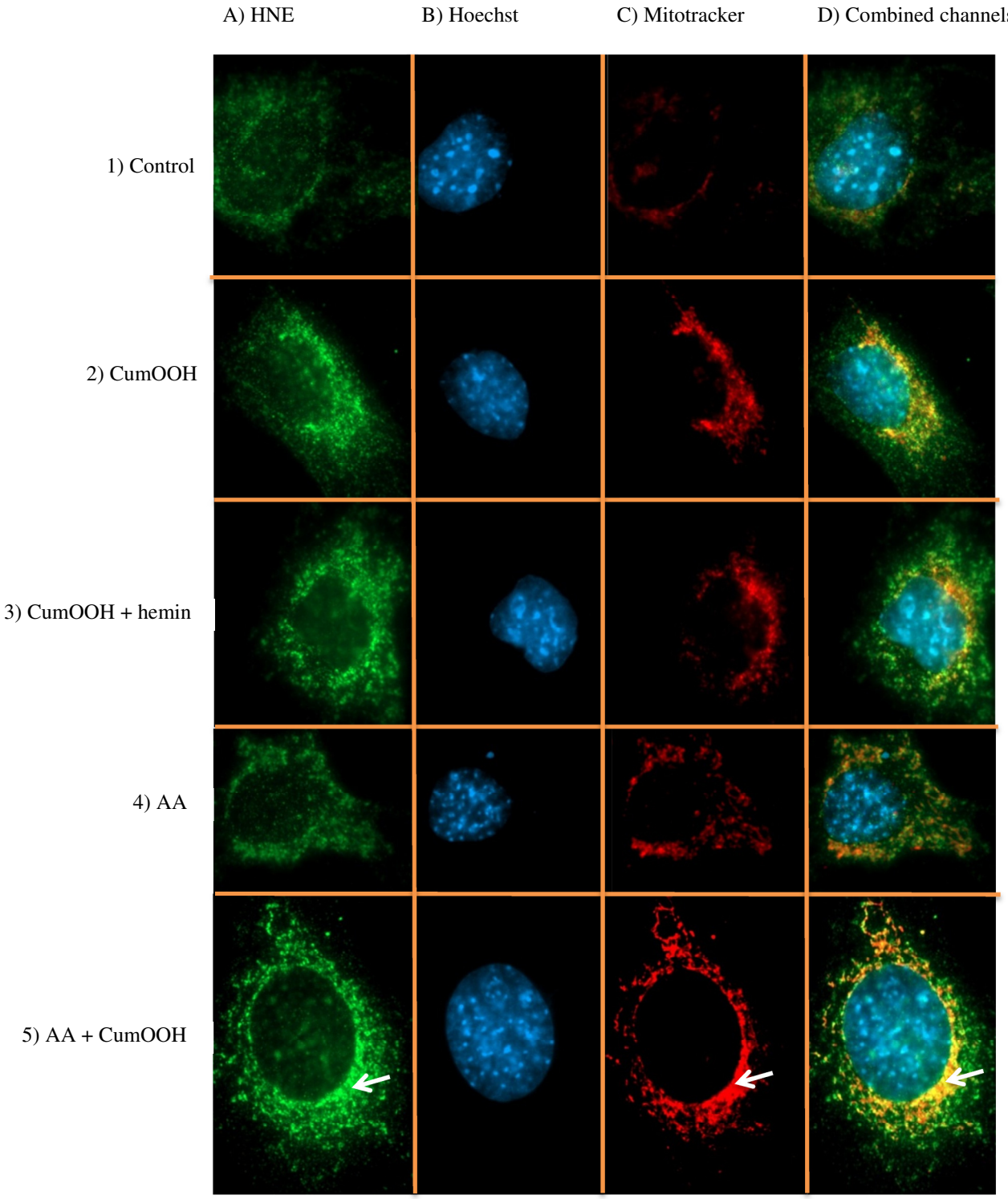

Figure 3.8: Immunocytochemical staining for histidine-HNE protein modifications with different treatments. *Cells were allowed to grow for 24 hours with or without 50 µM AA,and then treated with either nothing or 1 hour incubation with 80 nM hemin, followed by 30 minutes of incubation with or without 50 µM cumOOH. 1) Control without any treatments. 2) Treated with 50 µM cumOOH. 3) Treated with 50 µM cumOOH + 80 nM hemin, 4) Cells treated with 50 µM AA, 5) Cells treated with 50 µM AA +50 µM cumOOH. A) 4-HNE antibody. B) Hoechst 33342 staining, C) Mitotracker staining, D) A, B and C are laid on top of each other, showing DNA, mitochondria and 4-HNE adducts. The photos were taken with a 63x objective.*

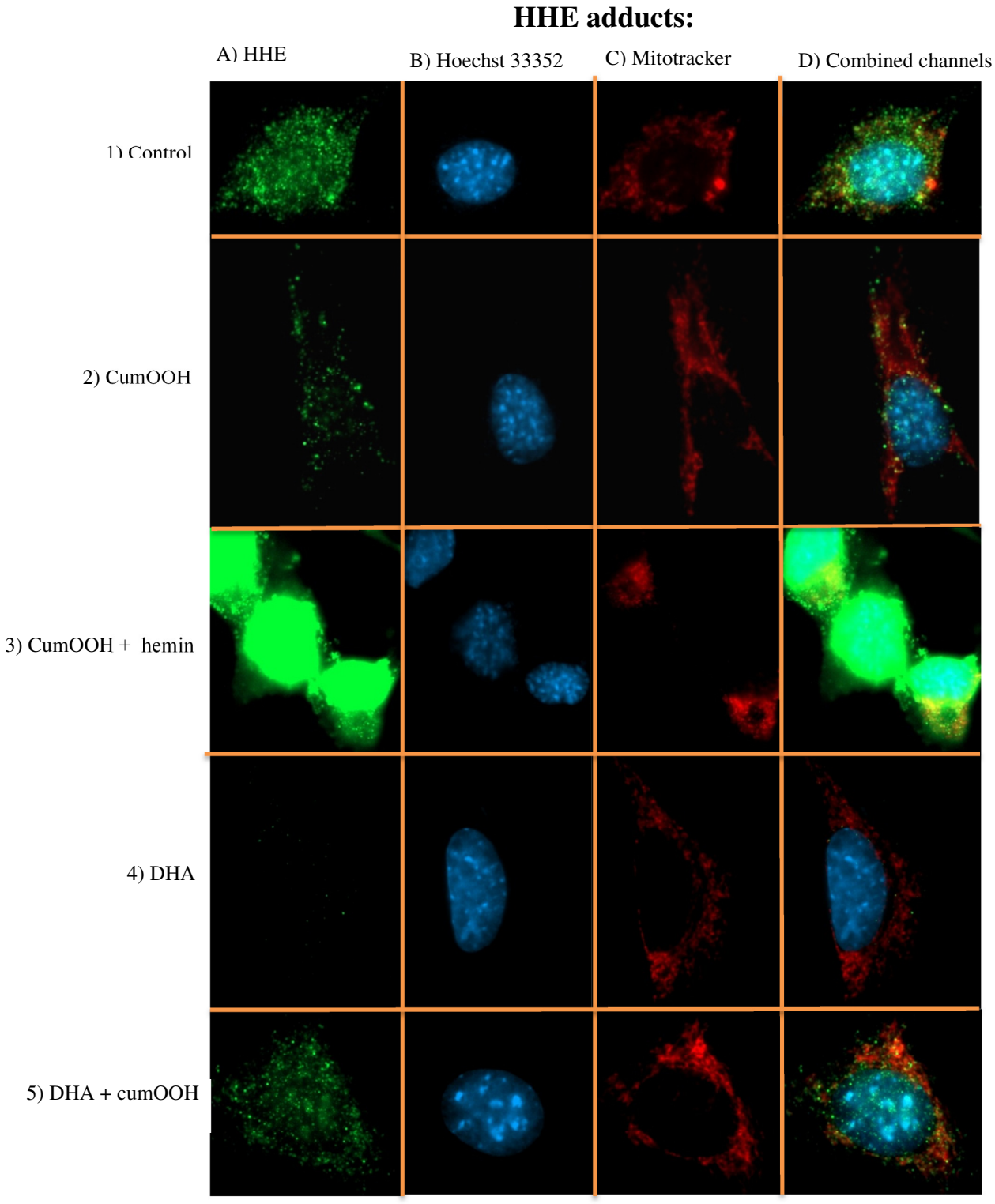

Figure 3.9: **A figure showing immunocytochemical staining for HHE protein modifications with different treatments.** *Cells were allowed to grow for 24 hours with or without 50 µM AA,and then treated with either nothing or 1 hour incubation with 80 nM hemin, followed by 30 minutes of incubation with or without 50 µM cumOOH. 1) Control without any treatments. 2) Treated with 50 µM cumOOH. 3) Treated with 50 µM cumOOH + 80 nM hemin., 4) Cells treated with 50 µM DHA, 5) Cells treated with 50 µM DHA +50 µM cumOOH. A) HHE antibody. B) Hoechst 33342 staining, C) Mitotracker staining, D) A, B and C are laid on top of each other, showing DNA, mitochondria and HHE adducts. The photos were taken with a 63x objective.*

3.2.1.3 HNE content in MEF-cells

In this part the aim was to quantify HNE adducts with AA + cumOOH-treated cells.

Cells were treated with three concentrations of AA (50, 75 and 100 µM) plus 2 controls (both without supplementation of AA, but one with 50 µM cumOOH) for 24 hours followed by incubation with 50 µM cumOOH for 30 minutes except for the negative control. The experimented was completed and protein lysates were prepared and protein concentration was adjusted to 0.05 µg/µL. The experiment was repeated three times. A control without secondary antibody in order to exclude endogenous peroxidase were also included in this test, it is not shown in the figure but can be found in the appendix A.3.2.

There were no statistical significant differences between the different treatment groups when compared with cumOOH (figure 3.10). A slight tendency was that AA gave lead to a decrease in HNE adduct formation. The data displayed a high run to run variation.

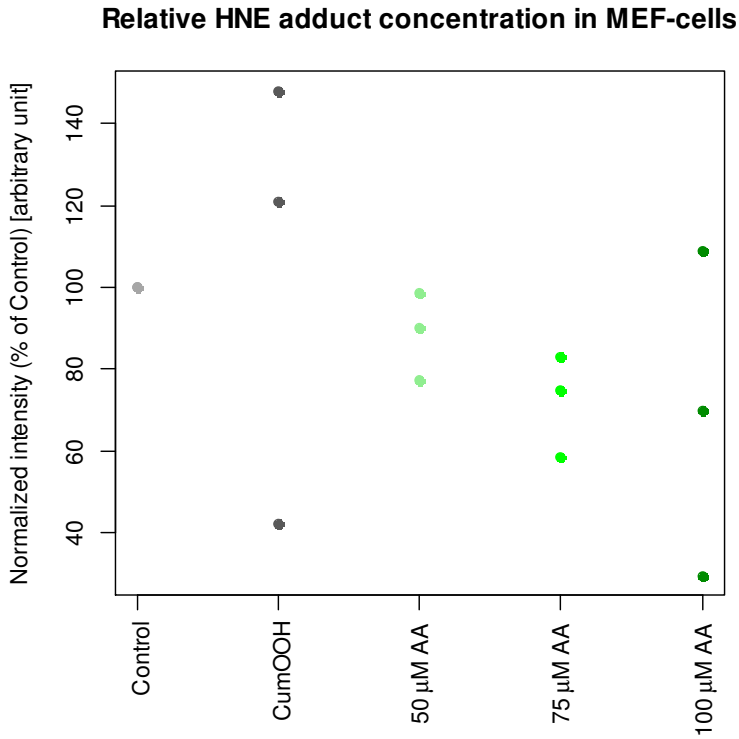

Figure 3.10: slot blot analysis for HNE adducts for MEF-cells after 24 hours of incubation with different concentrations of AA and two control. Every treatment received 50 µM cumOOH except the control. *The band intensity is on the y-axis and shown as % of control. The different treatments are on the x-axis. The experiment was done three times (n=3) with one technical replicate (zero parallels).*

3.2.2 *In vivo*: Oxidative stress in obese animals

3.2.2 Oxidative stress in a high fat induced obesity mouse model

In this last part we investigated the effects of a high fatty diet profile in mice, with protein carbonyls and HNE adducts as markers of oxidative stress. One group was fed with a diet consisting of 45 % fat, whereas the other was with a "normal" diet consisting of 10% fat. The mice were on a high fat diet for six weeks and are described more in section 2.3.

Obesity in humans and in experimental animals is associated with increased oxidative stress and the aim in this last part was to investigate the effects of oxidative stress markers of high fat diet induced obesity in mice.

We investigated protein carbonyl content in plasma, and in the fluid from caput epididymis and vas deferens. Plasma and epididymal fluids were chosen to avoid interference of naturally occurring carbonyls in nucleic acids. Epididymal fluid was included as spermatozoa are especially susceptible to damage by oxidative stress and the seminal fluid is rich in antioxidants.

Due to loss of three samples we only obtained 3 protein lysates from the control group in vas deferens (normal diet, n=3). For all other groups the sample size was 6 (n=6).

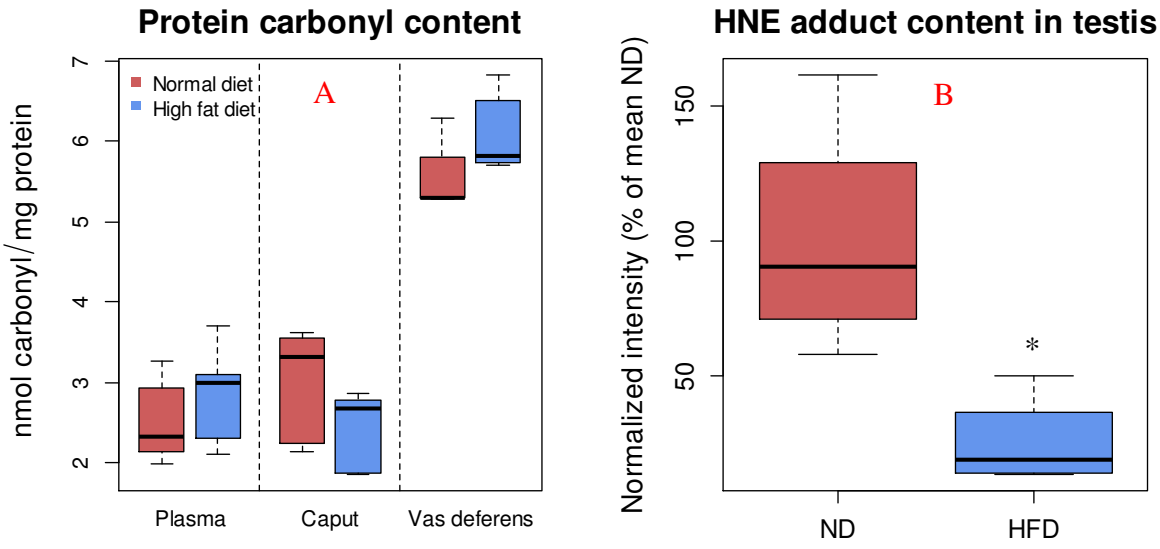

Figure 3.11: Protein carbonyl content in plasma, caput and vas deferens (A) and relative HNE adduct levels in testicular tissue (B) between mice on a high fatty diet, and mice on a normal diet. *A: The boxplots compares two groups of mice gone on either a high fat or a normal diet in plasma (n=6), caput (n=6) and vas deferens (n=3 and n=6 for normal diet and high fat diet, respectively). B: The boxplots shows lower values for the HFD-group (n=4) compared to the ND-group (n=4). *p < 0.05 statistically significant versus ND.*

We also examined HNE adducts in mice gone on a high fatty diet with mice gone on a normal diet. Due to a restricted availability of testicular tissue, the protein concentration were too low in some of the samples the sample size was thus reduced from 12 to 8, with 4 samples from the ND-group (n=4) and 4 samples from the HFD-group (n=4).

No differences were seen in protein carbonyl content between the two groups in plasma (p-value=0.11, Kruskal-Wallis test) and in the fluids from the vas deferens (p-value=0.20, Kruskal-Wallis test) and the caput epididmys (p-value=0.38, oneway-ANOVA) (figure 3.11 A).

Figure 3.11 B shows that mice on a high fatty diet has lower HNE adduct content compared to mice on a normal diet (oneway-ANOVA, $p<0.05$).

4 Discussion

ROS are present in all cells and are continuously introduced via endogenous or exogenous processes. ROS may act as messengers within a cell, but under environmental, chemical or nutritional stress the content of ROS can increase and eventually lead to a condition of oxidative stress by overwhelming the antioxidant defence in cells. Markers for detecting oxidative stress is important, as oxidative stress is known to be involved in a variety of medical conditions, including diabetes, cardiovascular diseases and obesity. The establishment of relevant, specific and robust biological markers for oxidative stress is important in order to detect damages before they develop into diseases.

4.1 Establishment of the methods

A main aim of this thesis was to establish methods to detect protein markers of oxidative stress that are applicable in archival tissues. In this first part of the discussion the focus is on the establishment of the methods. The establishment itself, as well as advantages and disadvantages regarding the methods are discussed.

4.1.1 CLPAA assay

The CLPAA assay was successfully established at the laboratory for both MEF-cells and Ntera-cells. The CLPAA assay was recently established (Hofer & Olsen, 2010), and has also been applied for testing out efficiency of antioxidants (Hofer et al., 2014). The method was easily established and we only did a single experiment to test it out. Moreover, it is cheap, time-efficient and allows a large number of different treatments. It is only applicable to live cells and was included to study effects of FA supplementation in cultured cells.

4.1.2 Detection of oxidized proteins with immunocyto- and histochemistry

In this thesis immunocyto- and histochemical methods were applied using primary antibodies toward protein modifications followed by fluorescent labelled secondary antibodies and attempts were made to quantify fluorescence intensity values. We were able to quantify fluorescence intensity values of Ntera-cells as they were rounded up, making it easy to circle them in using the ZEN software. However, when cells are in their natural conformation the quantification of fluorescence intensity values can be more challenging. We also observed that neighbouring cells may respond differently to the same treatment. This result in high variance and cells must be sampled to point out differences between treatment groups if they are to be treated statistically. Effective software and image analysis is therefore needed, which over the years has been developed.

Immunocyto- and histochemistry is extremely useful to localize specific antigens, which cannot be done by other methods such as western blotting and ELISA. By staining for several epitopes and/or cellular organelles subcellular localisation may be useful. For example, by staining a protein and a cellular organelle one can determine in which organelles the cells are localized (or where it is not localized). Subcellular localisation can be assessed subjectively

by simply looking at the mix of colors from the different fluorescent probes, as was done in this thesis. However, with the development of image analysis several approaches of these assessments can be done objectively (Dunn et al., 2011; Glynn & McAllister, 2006).

Protein carbonyls has for a long time been used as a marker of oxidative stress (Dalle-Donne, Rossi, et al., 2003). However, we experienced problems both *in vitro* and *in vivo* regarding detection of protein carbonyls by immunocyto- and histochemistry, respectively. We had high background issues, and were unable to distinguish between controls and H_2O_2-treated samples, although we were able to achieve somewhat of a dose-response curve *in vitro* in one of the experiments (3.1.2). It can possibly be explained by insufficient blocking of nonspecific staining. Insufficient blocking may allow binding of the mono or polyclonal antibody to bind to nonspecific sites, which may result in false positives. Alternatively, high background staining may be caused by interference from other carbonyl species in the cell.

When marking protein carbonyls with DNPH, it is important that the sample under investigation contains low concentrations of nucleic acids. Nucleic acids contain carbonyl groups and will react with DNPH, thereby possibly causing false positives.

4.1.3 Detection with ELISA and slot blot

We successfully developed the detection of HNE adducts by a slot blot analysis We had negligible background issues when applying samples without primary or secondary antibodies, which confirm that the anti HNE adduct antibody is specific, and that endogenous peroxidase was not a problem in our samples. We observed large differences between different runs in the *in vitro* experiments, and it is unknown if this is simply natural differences between cells. Several other papers have used dot blot (same method as slot blot) as a way to measure HNE adducts between various groups (Bradley et al., 2012; Jørgensen et al., 2014) and seemingly does not have the same problem. However, run-to-run variation is not a problem since it can be handled statistically by either normalizing the response variable for each run, or by using a general mixed model which takes run-to-run variation into account.

For the aging model it was expected from the literature that adult individuals had more HNE-adducts compared to young individuals. Increased concentrations of HNE adducts in older individuals has been shown in brain (Papaioannod et al., 2001), kidneys in rats (J. H. Lee et al., 2004), as well as *in vitro* in senescent fibroblasts (passage number=61) which had elevated HNE-concentrations (Jørgensen et al., 2014). Samples from young and aged animals were thus included to provide a control for the *in vivo* performance of the HNE slot blot assay. Although increased levels of HNE with age was observed, it was not statistical significant in the brain (p-value=0.08), this might be due to low sample size in the groups (n=3). A possible explanation for the variability observed in HNE adducts (figure 3.5) in brain was that a random part of the brain was taken out. Selection of a specific brain part was not possible as the whole brain was flattened, and a random part was therefore taken out. As the brain is a heterogeneous organ three replicates is probably not a sufficient sample size to overcome this variability.

For testis it was observed a statistical significant increase of HNE adduct in adult mice compared to young mice. Our results therefore suggest that HNE-adduct levels increases in testicular tissue with ageing. Previously it has been shown that testicular ageing involves mitochondrial dysfunction (Amaral et al., 2008). As oxidative stress is involved in the pathogenesis of testicular disorders and HNE-modified proteins as a marker of such has been shown to have elevated levels in testicular diseases, for example in varicocele (Shiraishi & Naito, 2005).

A weakness with the slot blot analysis in our lab was the difficulty of obtaining technical replicates because of the limited physical space on the nitrocellulose membrane when incubating with primary and secondary antibodies. It was difficult to acquire more than 24 spots for samples. If three technical replicates are wanted, then it follows that there are only room for 8 samples, and even less if establishing a standard curve is necessary. However, a better slot blot apparatus would allow more samples in the same run, and thereby improving the efficiency of the method.

4.2 Markers of Oxidative stress

In this thesis detection of several biological markers of oxidative stress was detected; C_{11}-bodipy, protein carbonyls, HHE and HNE adducts. An aim was to establish methods that could detect oxidative damage *in vitro* and in archival tissue.

Although protein carbonyl, HHE and HNE are known to be relevant in disease, we were able to detect differences in a physiological model of dietary, in which no pathological picture had yet taken place. This allows the study of not only overt oxidative stress in disease states, but also adaptive responses to ROS and involvement of oxidative stress in disease progression.

C_{11}-bodipy as a marker of lipid peroxidation can be beneficial because it can measure lipid peroxidation while cells are alive. This is advantageous in *in vitro* experiments as it provides a highly efficient possibility of examining effects of different toxicants, stressors and stress modifiers on lipid peroxidation. C_{11}-bodipy is an effective reporter molecule to measure the cells anti-lipidperoxdation capacity and a substance's ability to induce lipid peroxidation, and the reporter molecule was successfully applied in the assay to measure effects of fatty acid supplementation in this thesis. The peroxidation of the lipids themselves is not measured and requires other methods. A potential downside is that C_{11}-bodipy has been shown to overestimate the lipid peroxidation and also that it inhibits oxidative lipid damage (MacDonald et al., 2007). That it inhibits oxidative lipid damage is not surprising since the probe itself is being oxidized.

Protein carbonyls are a diverse group of oxidative protein damage, and are the most widely used biomarker for oxidative damage to proteins (Aldini et al., 2006). Protein carbonyls have been linked up to a variety of diseases including Alzheimer's, Parkinson's , diabetes, chronic renal failure and chronic lung disease (Dalle-Donne et al., 2003). However, the severity of the damage depends on the protein in question as some proteins are more critical for cellular

function. Also, some proteins are more susceptible than others for carbonyl formation. The degree of susceptibility depends on a variety of factors, including location, the presence of metals, sequences prone to carbonylation and nucleotide-binding proteins (Cabiscol et al., 2013). For example, in Alzheimer's disease superoxide dismutases (SOD1) are major targets of oxidative damage. However, only one of the four human brain SOD1 isoforms is heavily carbonylated (Choi et al., 2005). Moreover, which proteins that are susceptible to carbonylation is species dependent: Plasma in mice show an increase in carbonylation in transferrin and albumin, whereas plasma in rats show an increase in albumin and α1-macroglobulin (Jana et al., 2002).

The method for detecting protein carbonyls through labeling with DNPH is not specific as DNPH labels all ketones and aldehydes. This is the reason why nucleic acid content has to be low as DNA and RNA contains natural aldehydes. Protein carbonyls are not specific markers since it can affect nearly all proteins (Berlett & Stadtman, 1997). Moreover, determining the exact cause of formation of protein carbonyls is difficult as they can be formed either through the attack of ROS, or through attacks from secondary generated aldehydes such as HNE and HHE (Berlett & Stadtman, 1997).

Both HNE and HHE adducts are more specific markers compared to protein carbonyls, and reflect more of what type of stress the cells have been exposed to. HHE and especially HNE have been linked up to numerous diseases as explained in the introduction (section 1.4.2). HHE and HNE are lipid peroxidation derived aldehydes of omega-3 and omega-6 respectively. It is thus not surprising that these markers have been found in PUFA rich tissues such as the brain and testis. As with protein carbonyls, the cellular consequences of the damage depend on the protein being modified. In this thesis slot blot was used for detecting HNE adducts and this method gives a measure of the cellular amount of HNE-modified protein but does not allow detection of which proteins that were modified. A gel-electrophoreses/western blot includes protein separation and ultimately allows identification HNE- and HHE modified proteins according to size. Proteomic tools such as mass spectrometry and protein microassays that allows for more precise detection of modified proteins have recently been applied for studies of oxidized proteins in ageing and disease (Fritz et al., 2012).

HHE as biological marker of lipid peroxidation has over the last year received more attention and as monoclonal antibodies have been developed (Yamada et al., 2004), their involvement in diseases are arising (section 1.4.2). They might be of greater importance in omega-3 rich tissues such as the retina and brain compared to HNE.

An alternative to HNE as markers of lipid peroxidation are F_2-isoprostanes, which are prostaglandin-like substances formed from peroxidation of arachidonic acid and have been shown to be promising markers of endogenous lipid peroxidation. They have been suggested to increase in normal mice and humans with age (Milne et al., 2005), obesity (Vincent & Taylor, 2006) and a variety of diseases including cancer (Rossner et al., 2006), Alzheimer's

(Montine et al., 1998), Parkinson's (Seet et al., 2010) and diabetes (Gopaul et al., 2001). They are distributed throughout the body and they are chemically stable in archival tissue if stored at -80°C. However, only gas chromatography-mass chromatography and liquid chromatography-mass spectrometry have been proven to viable for measurement of F_2-isoprostanes, as immunoassays can be confounded with other similar molecules such as cyxooxygenase-derived prostaglandins (Milne et al., 2015; Soffler et al., 2010).

4.3 Cell culture study: Oxidative stress and effects of different types of fatty acids

Due to the simplicity of cellular cancer lines compared to in vivo models, they cannot reproduce the complex interactions that take place within an intact organism, and extrapolation of *in vitro* is therefore difficult, and should be done carefully. However, cell line studies can provide valuable mechanistic information of what happens when a substance is introduced into a biological system. Moreover, the search for better in vitro models (e.g 3D culture models) is on-going, as it is important to attempt to reduce the use of experimental animals.

4.3.1 Lipid peroxidation rates

The aim was to see if supplementing cell cultures with fatty acids would have an effect on lipid peroxidation. The CLPAA assay is an indirect method for measuring lipid peroxidation, and what we are measuring is the probe itself, it does not provide evidence that the cellular membranes themselves are being oxidized.

In the first part we investigated if fatty acids could act as scavengers when cells were also treated with an inducer of lipid peroxidation, namely cumene hydroperoxide (cumOOH). The PUFAs arachidonic acid (AA) and docosahexaenoic acid (DHA) proved to effective scavengers by reducing the lipid peroxidation of C11-bodipy. DHA was effective at all concentrations, whereas AA was effective at 50 μM and 100 μM. These results are consistent of what have been shown before. Richard et al., (2008) showed that eicasapentaenoic acid (EPA) and DHA had the ability to scavenge O2•-, but they did not test if AA could do the same, and concluded that EPA and DHA acts as antioxidants. It is not farfetched to believe that AA also has the ability to scavenge radicals, as they are readily attacked by radicals. However, uncontrolled lipid peroxidation produces even more radicals and also reactive aldehydes, so even if they have the ability to scavenge ROS it may ultimately increase the oxidative stress. More surprisingly was that palmitic acid (PA) appeared to have an antioxidant effect at 100 μM. Even though PUFAs are more susceptible to lipid peroxidation than saturated fatty acids, saturated fatty acids such as PA may be oxidized forming hydroxylated PAs (Truan & Peterson, 1998).
In the second part we investigated if fatty acids could have an effect on lipid peroxidation without the presence of a stressor. We wanted to measure whether the baseline lipid peroxidation would change when cells had been pre-treated with fatty acids. The CLPAA assay showed that the lowest concentration of 25 μM AA after 24 hours had a significant increase in oxidation of C11-bodipy compared to the control. Although not significant for the

other treatments, the oxidation of C11-bodipy in the control (not treated with fatty acids) was slightly lower than all the other treatments. Based on the first lipid peroxidation rate experiment (part 1) we expected that the higher amounts of polyunsaturated fatty acids in the treatments groups would decrease the lipid peroxidation of the C11-bodipy. This is because the PUFAs would be oxidized rather than the probe.

4.3.2 HNE and HHE adducts

It must be emphasized that we did not quantify fluorescence intensity values for HNE and HHE adducts. It was difficult to assess the results since the cells in these studies showed large differences in response to the same treatment.

4.3.2.1 HNE and HHE adducts

The HNE adducts did seem to give a stronger signal for the cumooh and cumooh + hemin treated cells compared to the control. The AA-treated cells seem to give an increase in fluorescence intensity, however, treating it with both AA and cumOOH gave an apparent increase compared to the cells only treated with cumOOH. This is consistent in what was shown by the CLPAA assay and that AA in the cells is being oxidized when treated with a stressor. As with HHE, HNE can diffuse across cellular membranes, forming adducts throughout the cells. Based on our investigation, the HNE adducts was found to a higher extent outside the cell nucleus, and at least for some of the pictures showed subcellular localization with mitochondria, which has been shown before (Usatyuk et al., 2006). Usatyuk et al., (2008) also shows that HNE adducts are mostly located outside the cell nucleus.

In the slot blot analysis it was observed no differences between the different groups. We expected increased levels of HNE adducts when cells were treated with AA + cumOOH compared to cells being only treated with cumOOH. One reason being that omega-6 in itself is prone to oxidation, another reason is because AA induces pro-inflammatary pathways such as interleukin-1 (IL-1) and tumor necrosis factor-alpha (TNF-α) (Rizzo & Carlo-Stella, 1996), which may ultimately result in oxidative stress and therefore also higher concentrations of HNE.

Based on the *in vitro* CLPAA assay we expected there to be differences in the slot blot analysis when cells were treated with either omega-6 or cumOOH, only cumOOH or simply no treatment. Why it was not observed more differences is difficult to explain. A possible explanation is that different cell types were used on the first part of the CLPAA assay and the slot blot analysis. MEF-cells might be more robust to lipid peroxidation compared to Ntera-cells, so that fewer aldehydes are produced under stress. However, the MEF-cells did show a significant increase in cumOOH induced oxidation of the C_{11}-probe. Another possible explanation might be that even though the fatty acids were oxidized, other aldehydes than HNE was formed, forming other adducts on cellular macromolecules. All of these adducts are not detected by the HNEJ-2 monoclonal antibody as it is highly specific for HNE-histidine Michael adducts (Toyokuni et al., 1995). Moreover, HNE does not only form Michael histidine adducts, but also Michael lysine and cysteine adducts, as well as reacting with the ε-amino group of lysine forming a Schiff base (Dalleau et al., 2013).

Overall the HHE adducts seemed to be more concentrated within the cell nucleus compared to the HNE adducts. Moreover, our pictures indicate that colocalization with mitochondria was more valid for HNE adducts compared to HHE adducts. Both these observations can possibly be explained by that HNE is more reactive than HHE (Bacot et al., 2003), which would allow HNE to react more rapidly and not diffuse throughout the cell. It has been shown *in vivo* that ischemia induces HNE adducts along with a decrease in GSH in mitochondria (Chen et al., 2001)

4.3.2.2 HHE-adducts

An objective was to localize the adducts and determine whether they were inside or outside the nucleus or if they are co-localized with the mitochondria. The adducts were mostly in the cytosol, and to some degree they were found within the mitochondria. Because of the natural production of ROS in mitochondria (Andreyev et al., 2005; Balaban et al., 2005), it is expected that the adducts to some extent is located around the mitochondria. However, the adducts have the ability to diffuse through cellular compartments and form adducts with DNA (Winter et al., 1986), Ethanolamine phospholipids (Bacot et al., 2007) and proteins (Long et al., 2008).

4.4 High fat diet over six weeks, a danger free zone?

This last study was part of a larger study examining the possible relationship between high fat diet induced obesity and impaired sperm quality. Oxidative damages is involved in reduced fertility seen in men (Gharagozloo & Aitken, 2011). Our hypothesis was that levels of oxidative stress is higher in obese than in control mice.

Our results show that no differences between protein carbonyl content between groups on a high fat diet and group on a normal diet. The slot blot analysis revealed that the testis had fewer HNE adducts in the mice fed on a high fat diet compared to mice fed on a normal diet. This was the opposite of what we hypothesized. It has previously been shown that a high fat diet over nine weeks induces the generation of ROS in motile spermatozoa, increased DNA damage in sperm, reduced sperm motility as well as a reduction of testosterone levels (Bakos et al., 2011). Spermatozoa and the testis itself has high contents of polyunsaturated fatty acids (Alvarez & Storey, 1995), and Alvarez & Story hypothesized that elevated levels of ROS induces lipid peroxidation in spermatozoa, which in turn impairs sperm quality. A high fat diet in mice generally induces oxidative stress and impairs sperm quality in obese mice (Bakos et al., 2011; Duale et al., 2014). However, mice in these two studies were on a high fat diet over 9-11 weeks, which is a period that is known to induce insulin-resistance, diabetes, lower levels of testosterone and obesity. Obesity leads to increased content of adipose tissue. Aromatase cytochrome P450 enzyme is located in adipose tissue and the enzyme is responsible for converting testosterone to estrogen (Meinhardt & Mullis, 2002) and adipose tissue can also decrease testosterone production from Leydig cells (Caprio et al., 1999). Finally, adipose tissue can cause elevated temperature of the testicles which causes reduced sperm quality (Paul et al., 2008; Shiraishi et al., 2010). It is therefore suggested that the

lowered testosterone level is caused by an increase in adipose tissue in mice. Mice used in this experiment was on a high fat diet for six weeks, and during this period they did not develop diseases such as diabetes and insulin resistance. Even though the mice in this study gained weight, it is possible that six weeks on a high fat diet is not a sufficient time to increase the adipose tissue content to a level in which a decrease of reproductive function is seen. In this study it is also shown an increased expression of anti-oxidant genes (B. Lindeman, Norwegian Institute of Public Health, personal communication March 2015), which may be an adaptive response. Taken together this may explain the reduced oxidative damage seen in mice which was on a high fat diet for six weeks.

4.5 Conclusions

In this thesis we have successfully developed promising methods for detecting biomarkers of oxidative stress. The usage of the monoclonal antibodies directed against 4-HNE and 4-HHE histidine adducts are promising, both in fluorescence microscopy and for 4-HNE in a slot blot analysis. The CLPAA assay with C_{11}-bodipy as a reporter molecule seems promising for measuring lipid peroxidation, even though the method is indicative. We were not able to optimize protein carbonyls as markers when applying fluorescence microscopy due to sensitivity and background problems, but this might be further optimized in future research. However, background problems with protein carbonyls might not be possible to resolve due to their natural presence in cells.

We found that PUFA supplemented cells possibility has the ability to act as scavengers when ROS are present. However, cells supplemented with omega-6 and treated with a stressor did not seem to induce the formation of HNE *in vitro*. A high fat diet over six weeks in mice seems to protect against the formation of HNE in testis.

4.6 Methodological considerations

During this thesis we switched from Ntera-cells to MEF-cells for the *in vitro* studies. Due to high passage numbers of the Ntera-cells a new batch of cells was needed for the subsequent experiments. However, due to problems with the viability and growth of new batches of Ntera-cells, we were not able to get new cells up and going and therefore switched to MEF-cells. Ideally all the experiments should have been performed using one of the cell lines exclusively, unless the aim was to compare effects on different cell lines. Due to time pressure it was impossible to repeat all the experiments performed using the Ntera-cells using MEF-cells. Moreover, an apoptosis assay could have been applied to the cells to see if the fatty acid themselves have a toxic effect. Although cells were controlled by investigating them under a microscope, this is not a sufficient way to determine toxic effects of FAs, and it has been shown that some cell types are more prone to the toxicity of supplement of fatty acids than other types (Nøding et al., 1998).

A problem with the experimental design is that we assumed that the cultured cells would take up the fatty acids without actually doing a lipid content analysis of the cellular membranes. A

fatty acid analysis of the lipids could have been done performed with a capillary gas liquid chromatography (Brand et al., 2010). Unfortunately, we did not have the resources to do this, but cultured cells have been shown to take up fatty acids when added to the medium, including EA hy 926 (Tardivel et al., 2009), oligodendroglial OLN-93 cells (Brand et al., 2010) and five other cell types (Nøding et al., 1998). Moreover, our cultured cells were grown in 10% FCS which contains fatty acids, meaning that we added fatty acids to a system that already had fatty acids in its system. The exact composition of lipids in FCS is unknown and differs depending on the batch. However, saturated fatty acids are generally high and DHA and AA is generally low (Lagarde et al., 1984) compared to what is found in plasma in humans (Hodson et al., 2008).

4.7 Future work

A natural follow-up from this study is to finish the establishment of anti HHE antibody in immunocytochemistry, and also applying and establishing HHE and anti HNE antibodies for immunohistochemistry.

References

Alamdari, D. H., Kostidou, E., Paletas, K., Sarigianni, M., Konstas, A. G. P., Karapiperidou, A., & Koliakos, G. (2005). High sensitivity enzyme-linked immunosorbent assay (ELISA) method for measuring protein carbonyl in samples with low amounts of protein. *Free Radical Biology & Medicine*, 39(10), 1362–1367.

Aldini, G., Carini, M., Colombo, R., Rossi, R., & Milzani, A. (2006). Protein carbonylation, cellular dysfunction, and disease progression. *Journal of Cellular and Molecular Medicine*, 10(2), 389–406.

Alvarez, J. G., & Storey, B. T. (1995). Differential incorporation of fatty acids into and peroxidative loss of fatty acids from phospholipids of human spermatozoa. *Molecular Reproduction and Development*, 42, 334–346.

Amaral, S., Mota, P., Rodrigues, A. S., Martins, L., Oliveira, P. J., & Ramalho-Santos, J. (2008). Testicular aging involves mitochondrial dysfunction as well as an increase in UCP2 levels and proton leak. *FEBS Letters*, 582, 4191–4196.

Andreyev, A. Y., Kushnareva, Y. E., & Starkov, A. A. (2005). Mitochondrial metabolism of reactive oxygen species. *Biochemistry (Moscow)*, 70(2), 200–214.

Atkinson A.J., J., Colburn, W. A., DeGruttola, V. G., DeMets, D. L., Downing, G. J., Hoth, D. F., Oates, J. A., Peck, C. C., Schooley, R. T., Spilker, B. A., Woodcock, J., & Zeger, S. L. (2001). Biomarkers and surrogate endpoints: Preferred definitions and conceptual framework. *Clinical Pharmacology and Therapeutics*, 69(3), 89–95.

Bacot, S., Bernoud-Hubac, N., Baddas, N., Chantegrel, B., Deshayes, C., Doutheau, A., Lagarde, M., & Guichardant, M. (2003). Covalent binding of hydroxy-alkenals 4-HDDE, 4-HHE, and 4-HNE to ethanolamine phospholipid subclasses. *Journal of Lipid Research*, 44, 917–926.

Bacot, S., Bernoud-Hubac, N., Chantegrel, B., Deshayes, C., Doutheau, A., Ponsin, G., Lagarde, M., & Guichardant, M. (2007). Evidence for in situ ethanolamine phospholipid adducts with hydroxy-alkenals. *Journal of Lipid Research*, 48, 816–825.

Bakos, H. W., Mitchell, M., Setchell, B. P., & Lane, M. (2011). The effect of paternal diet-induced obesity on sperm function and fertilization in a mouse model. *International Journal of Andrology*, 34, 402–410.

Balaban, R. S., Nemoto, S., & Finkel, T. (2005). Mitochondria, oxidants, and aging. *Cell*, 120, 483–495.

Baylin, A., Kabagambe, E. K., Siles, X., & Campos, H. (2002). Adipose tissue biomarkers of fatty acid intake. *The American Journal of Clinical Nutrition*, 76, 750–757.

Beal, M. F. (2002). Oxidatively modified proteins in aging and disease. *Free Radical Biology and Medicine*, 32(9), 797–803.

Benedetti, A., Comporti, M., & Esterbauer, H. (1980). Identification of 4-hydroxynonenal as a cytotoxic product originating from the peroxidation of liver microsomal lipids. *Biochimica Et Biophysica Acta*, 620, 281–296.

Berlett, B. S., & Stadtman, E. R. (1997). Protein oxidation in aging, disease, and oxidative stress. *The Journal of Biological Chemistry*, 272(33), 20313–20316.

Boisen, K. A., Main, K. M., Rajpert-De Meyts, E., & Skakkebaek, N. E. (2006). Are male reproductive disorders a common entity? The testicular dysgenesis syndrome. *Annals of the New York Academy of Sciences*, 948, 90–99.

Bonilla, D. L., Fan, Y.-Y., Chapkin, R. S., & McMurray, D. N. (2010). Transgenic mice enriched in omega-3 fatty acids are more susceptible to pulmonary tuberculosis: impaired resistance to tuberculosis in fat-1 mice. *The Journal of Infectious Diseases*, 201, 399–408.

Bradley, M. A., Xiong-Fister, S., Markesbery, W. R., & Lovell, M. A. (2012). Elevated 4-hydroxyhexenal in Alzheimer's disease (AD) progression. *Neurobiology of Aging*, 33, 1034–1044.

Brand, A., Bauer, N. G., Hallott, A., Goldbaum, O., Ghebremeskel, K., Reifen, R., & Richter-Landsberg, C. (2010). Membrane lipid modification by polyunsaturated fatty acids sensitizes oligodendroglial OLN-93 cells against oxidative stress and promotes up-regulation of heme oxygenase-1 (HSP32). *Journal of Neurochemistry*, 113, 465–476.

Butterfield, D. A., Swomley, A. M., & Sultana, R. (2013). Amyloid β-peptide (1–42)-induced oxidative stress in Alzheimer disease: Importance in disease pathogenesis and progression. *Antioxidants & Redox Signaling*, 19(8), 823–835.

Cabiscol, E., Tamarit, J., & Ros, J. (2013). Protein carbonylation: Proteomics, specificity and relevance to aging. *Mass Spectrometry Reviews*, 33, 21–48.

Calder, P. C. (2009). Polyunsaturated fatty acids and inflammatory processes: New twists in an old tale. *Biochimie*, 91, 791–795.

Caprio, M., Isidori, A. M., Carta, A. R., Moretti, C., Dufau, M. L., & Fabbri, A. (1999). Expression of functional leptin receptors in rodent Leydig cells. *Endocrinology*, 140(11), 4939–4947.

Catalá, A. (2006). An overview of lipid peroxidation with emphasis in outer segments of photoreceptors and the chemiluminescence assay. *The International Journal of Biochemistry & Cell Biology*, 38, 1482–1495.

Catalá, A. (2009). Lipid peroxidation of membrane phospholipids generates hydroxy-alkenals and oxidized phospholipids active in physiological and/or pathological conditions. *Chemistry and Physics of Lipids*, 157, 1–11.

Catalá, A. (2010). A synopsis of the process of lipid peroxidation since the discovery of the essential fatty acids. *Biochemical and Biophysical Research Communications*, 399, 318–323.

Chandel, N. S., Maltepe, E., Goldwasser, E., Mathieu, C. E., Simon, M. C., & Schumacker, P. T. (1998). Mitochondrial reactive oxygen species trigger hypoxia-induced transcription. *Cell Biology*, 95, 11715–11720.

Chen, J., Henderson, G. I., & Freeman, G. L. (2001). Role of 4-hydroxynonenal in modification of cytochrome c oxidase in ischemia/reperfused rat heart. *Journal of Molecular and Cellular Cardiology*, 33, 1919–1927.

Choi, J., Rees, H. D., Weintraub, S. T., Levey, A. I., Chin, L. S., & Li, L. (2005). Oxidative modifications and aggregation of Cu,Zn-superoxide dismutase associated with Alzheimer and Parkinson diseases. *Journal of Biological Chemistry*, 280(12), 11648–11655.

Dalleau, S., Baradat, M., Guéraud, F., & Huc, L. (2013). Cell death and diseases related to oxidative stress: 4-hydroxynonenal (HNE) in the balance. *Cell Death and Differentiation*, 20, 1615–1630.

Dalle-Donne, I., Giustarini, D., Colombo, R., Rossi, R., & Milzani, A. (2003). Protein carbonylation in human diseases. *Trends in Molecular Medicine*, 9(4), 169–176.

Dalle-Donne, I., Rossi, R., Giustarini, D., Milzani, A., & Colombo, R. (2003). Protein carbonyl groups as biomarkers of oxidative stress. *Clinica Chimica Acta*, 329, 23–38.

Del Rio, D., Stewart, A. J., & Pellegrini, N. (2005). A review of recent studies on malondialdehyde as toxic molecule and biological marker of oxidative stress. *Nutrition, Metabolism and Cardiovascular Diseases*, 15, 316–328.

Drummen, G. P. C., Van Liebergen, L. C. M., Den Kamp, J. A. F. O., & Post, J. A. (2002). C11-BODIPY 581/591, an oxidation-sensitive fluorescent lipid peroxidation probe: (micro)spectroscopic characterization and validation of methodology. *Free Radical Biology & Medicine*, 33(4), 473–490.

Duale, N., Steffensen, I.-L., Andersen, J., Brevik, A., Brunborg, G., & Lindeman, B. (2014). Impaired sperm chromatin integrity in obese mice. *Andrology*, 2, 234–243.

Dunn, K. W., Kamocka, M. M., & McDonald, J. H. (2011). A practical guide to evaluating colocalization in biological microscopy. *American Journal of Physiology. Cell Physiology*, 300, C723–C742.

Fernández-Sánchez, A., Madrigal-Santillán, E., Bautista, M., Esquivel-Soto, J., Morales-González, A., Esquivel-Chirino, C., Durante-Montiel, I., Sánchez-Rivera, G., Valadez-Vega, C., & Morales-González, J. A. (2011). Inflammation, oxidative stress, and obesity. *International Journal of Molecular Sciences*, 12, 3117–3132.

Fritz, K. S., Kellersberger, K. A., Gomez, J. D., & Petersen, D. R. (2012). 4-HNE adduct stability characterized by collision-induced dissociation and electron transfer dissociation Mass spectrometry. *Chemical Research in Toxicology*, 25, 965–970.

Gharagozloo, P., & Aitken, R. J. (2011). The role of sperm oxidative stress in male infertility and the significance of oral antioxidant therapy. *Human Reproduction*, 26(7), 1628–1640.

Glynn, M. W., & McAllister, A. K. (2006). Immunocytochemistry and quantification of protein colocalization in cultured neurons. *Nature Protocols*, 1(3), 1287–1296.

Gopaul, N. K., Manraj, M. D., Hébé, A., Lee Kwai Yah, S., Johnston, A., Carrier, M. J., & Änggård, E. E. (2001). Oxidative stress could precede endothelial dysfunction and insulin resistance in Indian Mauritians with impaired glucose metabolism. *Diabetologia*, 44, 706–712.

Halliwell, B. (2007). *Free radicals in biology and medicine* (4th ed.). Oxford University Press.

Hammoud, A. O., Meikle, A. W., Reis, L. O., Gibson, M., Peterson, C. M., & Carrell, D. T. (2012). Obesity and male infertility: A practical approach. *Seminars in Reproductive Medicine*, 30, 486–495.

Hayflick, L. (2007). Biological aging is no longer an unsolved problem. *Annals of the New York Academy of Sciences*, 1100, 1–13.

Ho, E., Karimi Galougahi, K., Liu, C.-C., Bhindi, R., & Figtree, G. A. (2013). Biological markers of oxidative stress: Applications to cardiovascular research and practice. *Redox Biology*, 1, 483–491.

Hodson, L., Skeaff, C. M., & Fielding, B. A. (2008). Fatty acid composition of adipose tissue and blood in humans and its use as a biomarker of dietary intake. *Progress in Lipid Research*, 47, 348–380.

Hofer, T., Jørgensen, T. Ø., & Olsen, R. L. (2014). Comparison of food antioxidants and iron chelators in two cellular free radical assays: strong protection by luteolin. *Journal of Agricultural and Food Chemistry*, 62, 8402–8410.

Hofer, T., & Olsen, R. L. (2010). Cellebasert metode for måling av lipidperoksidasjon og antioksidantaktivitet. *Bioingenøren*, 10, 6–12.

Jana, C. K., Das, N., & Sohal, R. S. (2002). Specificity of age-related carbonylation of plasma proteins in the mouse and rat. *Archives of Biochemistry and Biophysics*, 397(2), 433–439.

Jørgensen, P., Milkovic, L., Zarkovic, N., Waeg, G., & Rattan, S. I. S. (2014). Lipid peroxidation-derived 4-hydroxynonenal-modified proteins accumulate in human facial skin fibroblasts during ageing in vitro. *Biogerontology*, 15, 105–110.

Kohen, R., & Nyska, A. (2002). Oxidation of biological systems: Oxidative stress phenomena, antioxidants, redox reactions, and methods for their quantification. *Toxicologic Pathology*, 30(6), 620–650.

Lagarde, M., Sicard, B., Guichardant, M., Felisi, O., & Dechavanna, M. (1984). Fatty acid composition in native and cultured human endothelial cells. *In Vitro*, 20(1), 33–37.

Lee, J. H., Jung, K. J., Kim, J. W., Kim, H. J., Yu, B. P., & Chung, H. Y. (2004). Suppression of apoptosis by calorie restriction in aged kidney. *Experimental Gerontology*, 39, 1361–1368.

Lee, J. Y., Je, J. H., Jung, K. J., Yu, B. P., & Chung, H. Y. (2004). Induction of endothelial iNOS by 4-hydroxyhexenal through NF-κB activation. *Free Radical Biology and Medicine*, 37(4), 539–548.

Long, E. K., Murphy, T. C., Leiphon, L. J., Watt, J., Morrow, J. D., Milne, G. L., Howard, J. R. H., & Picklo, M. J. (2008). Trans-4-hydroxy-2-hexenal is a neurotoxic product of docosahexaenoic (22:6; n-3) acid oxidation. *Journal of Neurochemistry*, 105(3), 714–724.

MacDonald, M. L., Murray, I. V. J., & Axelsen, P. H. (2007). Mass spectrometric analysis demonstrates that BODIPY 581/591 C11 overestimates and inhibits oxidative lipid damage. *Free Radical Biology and Medicine*, 42, 1392–1397.

Majima, J. H., Nakanishi-Ueda, T., & Ozawa, T. (2002). 4-hydroxy-2-nonenal (4-HNE) staining by anti-HNE antibody. *Methods in Molecular Biology*, 196, 31–34.

Marquez-Quiñones, A., Cipak, A., Zarkovic, K., Fattel-Fazenda, S., Villa-Treviño, S., Waeg, G., Zarkovic, N., & Guéraud, F. (2010). HNE-protein adducts formation in different pre-carcinogenic stages of hepatitis in LEC rats. *Free Radical Research*, 44(2), 119–127.

Meinhardt, U., & Mullis, P. E. (2002). The essential role of the aromatase/P450arom. *Seminars in Reproductive Medicine*, 20(3), 277–284.

Milne, G. L., Dai, Q., & Roberts, L. J. (2015). The isoprostanes - 25 years later ☆. *Biochimia Et Biophysica Acta*, 1851, 433–445.

Milne, G. L., Musiek, E. S., & Morrow, J. D. (2005). F2-isoprostanes as markers of oxidative stress in vivo: an overview. *Biomarkers*, 10, 10–23.

Montine, T. J., Morrow, J. D., & Neurol, A. (1998). Cerebrospinal fluid - F2-isoprostane levels are increased in Alzheimer's disease. *Annals of Neurology*, 44, 410–413.

Nakagawa, F., Morino, K., Ugi, S., Ishikado, A., Kondo, K., Sato, D., Konno, S., Nemoto, K. I., Kusunoki, C., Sekine, O., Sunagawa, A., Kawamura, M., Inoue, N., Nishio, Y., & Maegawa, H. (2014). 4-Hydroxy hexenal derived from dietary n-3 polyunsaturated fatty acids induces anti-oxidative enzyme heme oxygenase-1 in multiple organs. *Biochemical and Biophysical Research Communications*, 443(3), 991–996.

Nyström, T. (2005). Role of oxidative carbonylation in protein quality control and senescence. *The EMBO Journal*, 24, 1311–1317.

Nøding, R., Schønberg, S. a, Krokan, H. E., & Bjerve, K. S. (1998). Effects of polyunsaturated fatty acids and their n-6 hydroperoxides on growth of five malignant cell lines and the significance of culture media. *Lipids*, 33(3), 285–293.

Oberley, T. D., Toyokuni, S., & Szweda, L. I. (1999). Localization of hydroxynonenal protein adducts in normal human kidney and selected human kidney cancers. *Free Radical Biology and Medicine*, 27, 695–703.

Palmer, N. O., Bakos, H. W., Fullston, T., & Lane, M. (2012). Impact of obesity on male fertility, sperm function and molecular composition. *Spermatogenesis*, 2(4), 253–263.

Papaioannod, N., Tooten, P. C. J., Ederen, A. M. Van, Bohl, J. R. E., Rofina, J., Tsangaris, T., & Gruys, E. (2001). Immunohistochemical investigation of the brain of aged dogs. I. Detection of neurofibrillary tangles and of 4-hydroxynonenal protein, an oxidative damage product, in senile plaques. *Amyloid: The Journal of Protein Folding Disorders*, 8, 11–21.

Paul, C., Murray, A. A., Spears, N., & Saunders, P. T. K. (2008). A single, mild, transient scrotal heat stress causes DNA damage, subfertility and impairs formation of blastocysts in mice. *Reproduction*, 136, 73–84.

Pizzimenti, S., Ciamporcero, E., Daga, M., Pettazzoni, P., Arcaro, A., Cetrangolo, G., Minelli, R., Dianzani, C., Lepore, A., Gentile, F., & Barrera, G. (2013). Interaction of aldehydes derived from lipid peroxidation and membrane proteins. *Frontiers in Physiology*, 4, 1–17.

Rejraji, H., Vernet, P., & Drevet, J. R. (2002). GPX5 is present in the mouse caput and cauda epididymidis lumen at three different locations. *Molecular Reproduction and Development*, 63, 96–103.

Richard, D., Kefi, K., Barbe, U., Bausero, P., & Visioli, F. (2008). Polyunsaturated fatty acids as antioxidants. *Pharmacological Research*, 57, 451–455.

Rizzo, M. T., & Carlo-Stella, C. (1996). Arachidonic acid mediates interleukin-1 and tumor necrosis factor-α-induced activation of the c-jun amino-terminal kinases in stromalcells. *Blood*, 88(10), 3792–3800.

Rossner, P., Gammon, M. D., Terry, M. B., Agrawal, M., Fang, F. Z., Teitelbaum, S. L., Eng, S. M., Gaudet, M. M., Neugut, A. I., & Santella, R. M. (2006). Relationship between urinary 15-F2t-isoprostane and 8-oxodeoxyguanosine levels and breast cancer risk. *Cancer Epidemiology Biomarkers and Prevention*, 15(4), 639–644.

Russel, R. (1999). Atherosclerosis - an inflammatory disease. *The New England Journal of Medicine*, 340(2), 115–126.

Saleh, R. A., & Agarwal, A. (2002). Oxidative stress and male infertility: From research bench to clinical practice. *Journal of Andrology*, 23(6), 737–752.

Seet, R. C. S., Lee, C. Y. J., Lim, E. C. H., Tan, J. J. H., Quek, A. M. L., Chong, W. L., Looi, W. F., Huang, S. H., Wang, H., Chan, Y. H., & Halliwell, B. (2010). Oxidative damage

in Parkinson disease: Measurement using accurate biomarkers. *Free Radical Biology and Medicine*, 48, 560–566.

Shiraishi, K., & Naito, K. (2005). Increased expression of Leydig cell haem oxygenase-1 preserves spermatogenesis in varicocele. *Human Reproduction*, 20(9), 2608–2613.

Shiraishi, K., Takihara, H., & Matsuyama, H. (2010). Elevated scrotal temperature, but not varicocele grade, reflects testicular oxidative stress-mediated apoptosis. *World Journal of Urology*, 28, 359–364.

Silverthorn, D. U., Ober, W. C., Garrison, C., Silverthorn, A. C., & Johnson, B. R. (2009). *Human Physiology: An integrated approach* (5th ed.). Pearson/Benjamin Cummings.

Simopoulos, A. P. (2002). The importance of the ratio of omega-6 / omega-3 essential fatty acids. *Biomedicine & Pharmacotherapy*, 56, 365–379.

Singh, R., Wang, Y., Schattenberg, J. M., Xiang, Y., & Czaja, M. J. (2009). Chronic oxidative stress sensitizes hepatocytes to death from 4-hydroxynonenal by JNK/c-Jun overactivation. *American Journal of Physiology. Gastrointestinal and Liver Physiology*, 297, 907–917.

Skakkebæk, N. E., Meyts, E. R., & Main, K. M. (2001). Testicular dysgenesis syndrome: An increasingly common developmental disorder with environmental aspects. *Human Reproduction*, 16(5), 972–978.

Soffler, C., Campbell, V. L., & Hassel, D. M. (2010). Measurement of urinary F2-isoprostanes as markers of in vivo lipid peroxidation: A comparison of enzyme immunoassays with gas chromatography-mass spectrometry in domestic animal species. *Journal of Veterinary Diagnostic Investigation*, 22, 200–209.

Spector, A. A. (1999). Essentiality of fatty acids. *Lipids*, 34, 1–3.

Stadtman, E. R. (1998). Protein oxidation in aging and age-related diseases. *Drug Metabolism Reviews*, 30(2), 225–243.

Stefek, M., Masarykova, M., & Benes, L. (1992). Inhibition of cumene hydroperoxide-induced lipid peroxidation by a novel pyridoindole antioxidant in rat liver microsomes. *Pharmacology & Toxicology*, 70, 407–411.

Sun, Q., Ma, J., Campos, H., Hankinson, S. E., & Hu, F. B. (2007). Comparison between plasma and erythrocyte fatty acid content as biomarkers of fatty acid intake in US women. *The American Journal of Clinical Nutrition*, 86, 74–81.

Tanito, M., Brush, R. S., Elliott, M. H., Wicker, L. D., Henry, K. R., & Anderson, R. E. (2009). High levels of retinal membrane docosahexaenoic acid increase susceptibility to stress-induced degeneration. *Journal of Lipid Research*, 50, 807–819.

Tardivel, S., Gousset-Dupont, A., Robert, V., Pourci, M.-L., Grynberg, A., & Lacour, B. (2009). Protective effects of EPA and deleterious effects of DHA on eNOS activity in Ea hy 926 cultured with lysophosphatidylcholine. *Lipids*, 44, 225–335.

Toyokuni, S., Miyake, N., Hiai, H., Hagiwara, M., Kawakishi, S., Osawa, T., & Uchida, K. (1995). The monoclonal antibody specific for the 4-hydroxy-2-nonenal histidine adduct. *FEBS Letters*, 359, 189–191.

Tremellen, K. (2008). Oxidative stress and male infertility - a clinical perspective. *Human Reproduction Update*, 14(3), 243–258.

Truan, G., & Peterson, J. A. (1998). Thr268 in substrate binding and catalysis in P450BM-3 1. *Archives of Biochemistry and Biophysics*, 349(1), 53–64.

Uauy, R., Hoffman, D. R., Peirano, P., Birch, D. G., & Birch, E. E. (2001). Essential fatty acids in visual and brain development. *Lipids*, 36(9), 885–895.

Usatyuk, P. V., Parinandi, N. L., & Natarajan, V. (2006). Redox regulation of 4-hydroxy-2-nonenal-mediated endothelial barrier dysfunction by focal adhesion, adherens, and tight junction proteins. *Journal of Biological Chemistry*, 281(46), 35554–35566.

Valavanidis, A., Vlachogianni, T., & Fiotakis, C. (2009). 8-hydroxy-2' -deoxyguanosine (8-OHdG): A critical biomarker of oxidative stress and carcinogenesis. *Journal of Environmental Science and Health*, 27, 120–139.

Van Kuijk, F. J. G. M., Holte, L. L., & Dratz, E. A. (1990). 4-Hydroxyhexenal: A lipid peroxidation product derived from oxidized docosahexaenoic acid. *Biochimica Et Biophysica Acta*, 1043, 116–118.

Vernet, P., Aitken, R. J., & Drevet, J. R. (2004). Antioxidant strategies in the epididymis. *Molecular and Cellular Endocrinology*, 216, 31–39.

Vincent, H. K., & Taylor, A. G. (2006). Biomarkers and potential mechanisms of obesity-induced oxidant stress in humans. *International Journal of Obesity*, 30, 400–418.

Vindis, C., Escargueil-Blanc, I., Elbaz, M., Marcheix, B., Grazide, M. H., Uchida, K., Salvayre, R., & Nègre-Salvayre, A. (2006). Desensitization of platelet-derived growth factor receptor-β by oxidized lipids in cascular cells and atherosclerotic lesions: Prevention by aldehyde scavengers. *Circulation Research*, 98, 785–792.

Winter, C. K., Segall, H. J., & Haddon, W. F. (1986). Formation of cyclic adducts of deoxyguanosine with the aldehydes trans -4-hydroxy-2-hexenal and trans -4-hydroxy-2-nonenal in vitro. *Cancer Research*, 46, 5682–5686.

Yamada, S., Funada, T., Shibata, N., Kobayashi, M., Kawai, Y., Tatsuda, E., Furuhata, A., & Uchida, K. (2004). Protein-bound 4-hydroxy-2-hexenal as a marker of oxidized n-3 polyunsaturated fatty acids. *Journal of Lipid Research*, 45, 626–634.

Yoritaka, A., Hattori, N., Uchida, K., Tanaka, M., Stadtman, E. R., & Mizuno, Y. (1996). Immunohistochemical detection of 4-hydroxynonenal protein adducts in Parkinson disease. *Proceedings of the National Academy of Sciences of the United States of America*, 93, 2696–2701.

Yousef, M. I., Abdallah, G. a., & Kamel, K. I. (2003). Effect of ascorbic acid and Vitamin E supplementation on semen quality and biochemical parameters of male rabbits. *Animal Reproduction Science*, 76, 99–111.

Appendix

Appendix A.1 Cell maintenance

A.1.1 Thawing and freezing for MEFs and Ntera-cl.d2 cells.

Thawing:

- **i.** A 15 ml tube with cell suspension was taken up from a nitrogen tank and thawed in a 37°C water bath for 2-3 minutes.
- **ii.** The cell suspension was gently transferred to a new tube containing 13 mL culture medium.
- **iii.** Cells were centrifuged at 400 g for five minutes. The supernatant was removed and 7 mL culture medium was added.
- **iv.** The cells were resuspended carefully and the suspension was pipetted to a 25 cm^2 flask.

Freezing:

- **i.** Confluent cells (~75%) were trypsinated according to the procedure described in steps in iv (A.1.2: Growth and passaging).
- **ii.** Cells were transferred to 1.8 mL cryotubes and centrifuged at 400 * g for 5 minutes at 8 °C. Cells were resuspended in growth medium containing 10% dimethyl sulfoxide (DMSO).
- **iii.** The cell suspension was transferred to cryotubes (1.8 mL) and kept at 4°C for 5 minutes.
- **iv.** The tubes were placed half way down the nitrogen tank for 3-4 hours, and were then immersed to liquid nitrogen.

A.1.2 Growth and passaging: MEFs and Ntera-cl.d2

After seeding approximately $2*10^6$ cells for the Ntera-cl.D2 line and $5*10^5$ for the MEF line in a 75 cm^2 flask the cells entered a lag period for about 24 hours, followed by exponential growth for the next 48 hours reaching confluence approximately 3-4 days after being seeded.

When cells reached confluence they were split by the following procedure. Every step was done in a sterile way by spraying equipment with 70% ethanol and using a sterile bench.

- **i** The growth medium was removed from the flask followed by two PBS washes. The PBS volume used was equal to the medium volume for each wash.
- **ii** To detach the cells from each other, 3 ml trypsin was added to the flask, quickly distributed and then immediately withdrawing 2 ml, leaving 1 ml trypsin left in the flask. This was followed by incubation for 4 minutes at 37°C degrees. The cells were released

from the bottom of the flask by tapping carefully on the sides of the flask. Cell detachment was controlled by looking at them under a microscope

iii The trypsin was inactivated by adding 4 + 5 ml growth medium. Thorough pipetting was necessary in order to separate the cells.

iv Cells were counted either by:

a) A hemocytometer (a Bürker chamber): 100 µL cell suspension was mixed with 100 µL tryphan blue, and then 10 µL of this mix was added to each side of the bürker chamber (total of 20 µL). Living cells were counted across ten squares followed by multiplication of the mean with $2*10^4$, giving the number of cells per milliliter, or

b) A cell counter (CASY Model TT): 50 µL of the cell suspension was added to 10 mL of filtered CasyTon buffer, and then measured by the cell counter. The viability and the cell concentration were noted.

v The appropriate cell suspension cell volume plus culture medium giving a total of 20 mL was pipetted to a new 75 cm^2 flask. The name of the cell line, passage number and date was noted on the flask and in a cell protocol book.

A.2 Protein carbonyls: immunohistochemistry, detailed protocol

Liver tissue from a sacrificed mouse was divided into 4 equal parts followed by incubation with 2 different concentrations of H_2O_2 (5 mM and 10 mM) in PBS plus a control containing only PBS at 37°C at room temperature for 30 minutes. The tissues were washed in PBS followed by fixation in methacarn for 24 hours at 4 °C. Tissues were paraffin-embedded (Histo Comp,Vogel) by using Shandon Excelsior ES (Life Technologies). The following program was used:

Step	Solution	Incubation time	Temperature
1	Alcohol 75%	60 minutes	30°C
2	Alcohol 90%	60 minutes	30°C
3	Alcohol 96%	60 minutes	30°C
4	Absolute Alcohol	60 minutes	30°C
5	Absolute Alcohol	60 minutes	30°C
6	Absolute Alcohol	60 minutes	30°C
7	Xylene	60 minutes	30°C
8	Xylene	90 minutes	30°C
9	Xylene	90 minutes	30°C
10	Wax	80 minutes	58°C
11	Wax	80 minutes	58°C
12	Wax	140 minutes	58°C

After paraffin-embedding the samples, a microtome (Microm HM 355S, Life Technologies) was used to cut 4 μM thin sections, followed by rehydration:

i. Immerse the slides in 100% ethanol 2 times for 10 minutes each.
ii. Immerse the slides in 95% ethanol for 5 minutes.
iii. Immerse the slides in 70% ethanol for 5 minutes.
iv. Immerse the slides in 50% ethanol for 5 minutes.
v. Rinse the slides with deionized H_2O.
vi. Rehydrate the slides with PBS buffer for 10 minutes. Drain the excess wash buffer.

100 μL of antigen retrieval buffer (Biocare Medical) was to each slide. A glass coverslip was placed on top of the slide and incubated in a steamer for 20 minutes. Slides were allowed to cool down for 15 minutes at room temperature. Tissue was washed by incubating it in 100 μL a TBS buffer 3 times for 5 minutes. Tissue was surrounded with a hydrophobic barrier using a barrier pen and dried for 2 minutes. 100 μL of the DNPH solution (10 μM) was added to each slide and then incubated for 30 minutes at room temperature. Slides were washed in PBS buffer 3 times for 5 minutes. For blocking 100 μL of the background punisher (Biocare medical) was added to each slide and incubated at room temperature for 10 minutes. Slides were incubated with 100 μL of freshly prepared anti-DNP primary antibody (1:200 in TBS buffer) and incubated in a humidified chamber overnight at 4°C, followed by washing in TBS buffer 3 times for five minutes. Slides were immersed dH_2O and mounting media (dakocytomation, Dako) to the sample and cover the slide with a plastic slip.

A.3 Antibody controls regarding protein carbonyls, HNE and HHE adducts

A.3.1 Protein carbonyls

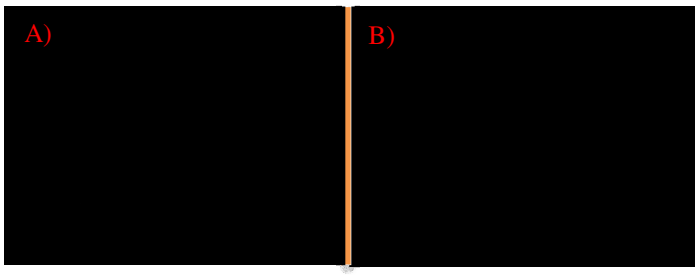

Figure A.3.1: Control for Anti-dinitrophenyl antibody and DNPH-control. A) Without primary antibody (with DNPH), B) Without DNPH (with primary antibody). They show no background. *The photos were taken with a 40x objective (400x magnification) on a Zeiss Axio Observer Z1 microscope.*

A.3.2: HHE and HNE adducts

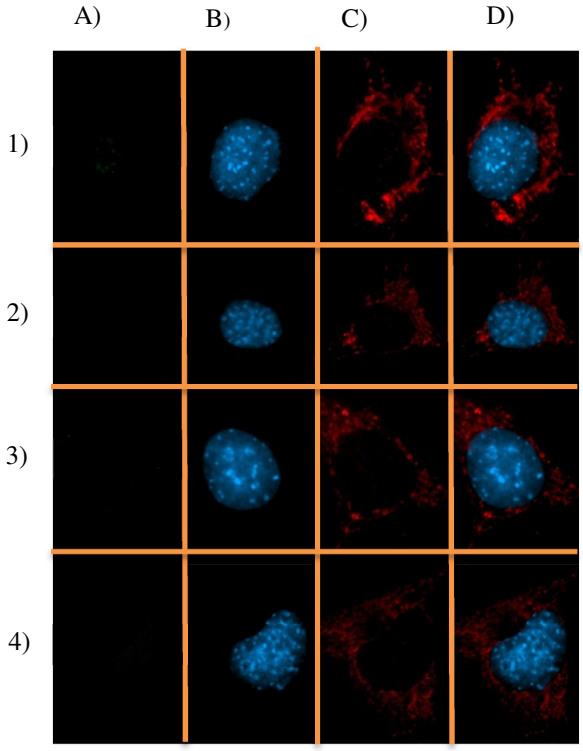

Figure A.3.2: Immunocytochemistry controls for the HHE and HNEantibodies: *1) A MEF not stained with primary antibody anti HHE, but with secondary antibody, 2) MEF stained with primary antibody, but without secondary antibody, 3) MEF not stained with primary antibody anti HNE, but with secondary antibody, 4) MEF stained with the primary antibody anti 4-HNE, but without secondary antibody. A) 4-HNE antibody. B) Hoechst 33342 staining, C) Mitotracker staining, D) A, B and C are laid on top of each other, showing DNA, mitochondria and HNE adducts. The photos were taken with a 63x objective.*

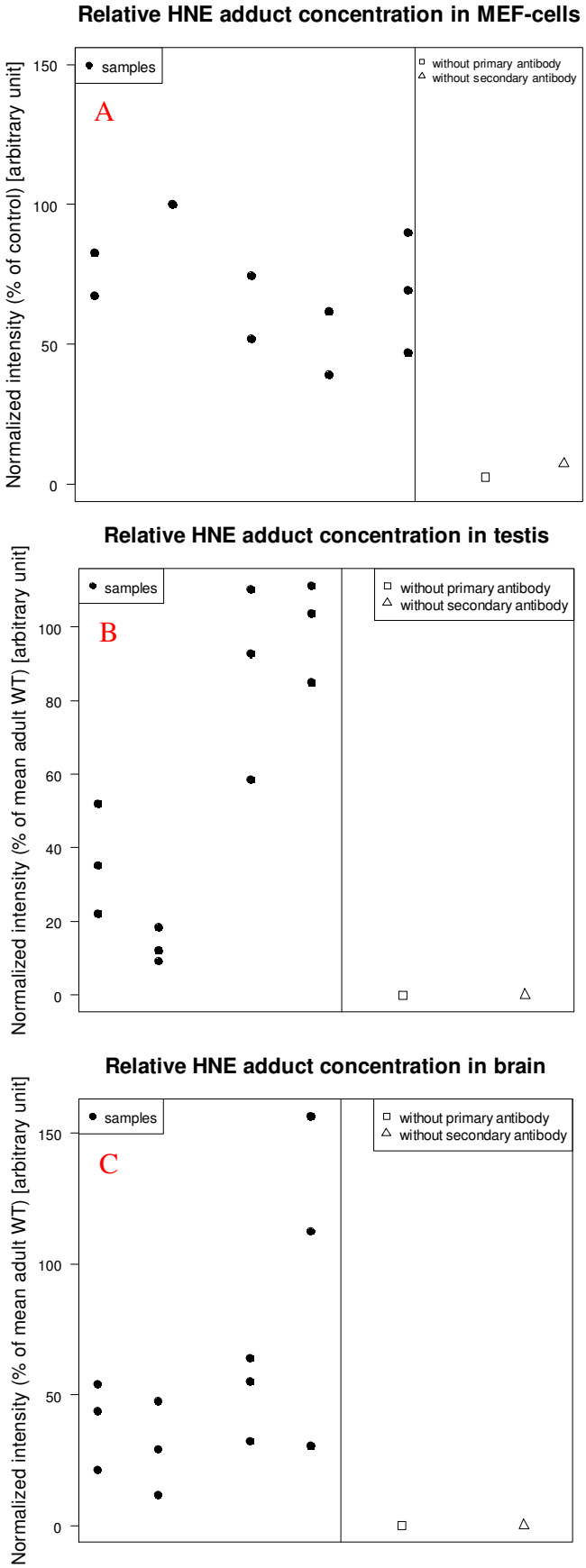

Figure A.3.3 Controls for the slot blot analysis for MEF-cells (A), testis (B) and brain (C). *The left side of line shows the samples from each experiment, and the right show two controls: One with primary antibody anti HNE, but without secondary antibody and one without primary antibody anti HNE, but with secondary antibodies. The x-axis labels were removed with intent. The controls show low background intensities.*

A.4 Solutions and buffers

Cumene hydroperoxide:
A stock solution of cumene hydroperoxide was prepared by adding 20 µL to PBS (gives 1.2 mL of 0.1 M). The working solution was made by adding 5 µL from this solution to 9995 µL of Hanks' solution. This was made immediately before use.

Growth medium for MEF-cells:
500 mL Dulbecco's Modified Eagle's Medium, with 4.5 g/L Glucose, without L-glutamine
55 mL (10%) Foetal Calf Serum
5.5 mL (1%) Penicillin-Streptomycin
5.5 mL (1%) L-Glutamine (200mM)

Growth medium for Ntera-2 cl.D1
500 mL Dulbecco's Modified Eagle's Medium, with 4.5 g/L Glucose, with L-glutamine, with Sodium Pyruvate
55 mL (10%) Foetal Calf Serum
5.5 mL (1%) Penicillin-Streptomycin

Treatment medium
500 mL Dulbecco's Modified Eagle's Medium, with 4.5 g/L Glucose, without L-glutamine
5.5 mL (1%) Penicillin-Streptomycin
5.5 mL (1%) L-Glutamine (200mM)

DNPH-solution
The solution was first prepared by making 50 mM stocks in phosphoric acid, which was stored at -20°C On the day of use, the stock was mixed with 40 mL of water. In order to make it more alkaline, NaOH was added until the pH was 6.2. This gives about 50 mL of a DNPH solution which can be used.

RIPA-buffer:
150 mM sodium chloride
1.0% Triton X-100
0.5% sodium deoxycholate
0.1% SDS (sodium docecyl sulphate)
50 mM Tris
Dissolved in dH_2O and pH adjusted to 8.0

TBS-buffer
50 mM Tris
0.15 mM NacL
Dissolved in dH_2O and pH adjusted to 7.6

A.5: Products and producers

Product	Producer	Country
2,4-Dinitrophenylhydrazine	Sigma-Aldrich	USA
Absolutt alcohol prima (100% (absolute) ethanol)	Kementyl	Norway
Acetic acid (glacial)	Merck	USA
Anti HHE monoclonal antibody	JaICA	Japan
Anti HNE monoclonal antibody (HNEJ-2)	JaICA	Japan
Anti-dinitrophenyl-KLH Alexa fluor 488	Life Technologies	USA
Axio observer Z1	Carl Zeizz	Germany
Background punisher	Biocare Medical	USA
BioWhittaker® Dulbecco's Modified Eagle's Medium, with 4.5 g/L glucose, without L-glutamine	Lonza	Belgium
BioWhittaker® Dulbecco's Modified Eagle's medium with 4,5 g/L glucose, with L-glutamine and with Sodium Pyruvate	Lonza	Belgium
BioWhittaker® L-glutamine 200mM	Lonza	Belgium
BioWhittaker® PEN-STREP (penicillin-streptomycin)	Lonza	Belgium
BioWhittaker® Trypan Blue 0.4%	Lonza	Belgium
BioWhittaker® Trypsin EDTA	Lonza	Belgium
Bovine Serum Albumin, Fraction V	Sigma-Aldrich	USA
Bodipy® 581/591 C11	Life Technologies	USA
CASY Model TT – Cell Counter and Analzyzer	Roche	Germany
CLARIOstar	Labtech	Germany

Centrifuge tubes 15 mL	Corning	USA
Centrifuge tubes 50 mL	Corning	USA
ChemiDoc™ XRS+	Bio-Rad	USA
Chloroform	Merck	USA
cOmplete, Mini, EDTA-free	Roche	
Corning flasks (75 cm^2, 162 cm^2)	Corning	USA
Costar Assay Plate 96 well Black with clear bottom	Corning	USA
Cumene hydroperoxide	Sigma-Aldrich	USA
Distilled water (dH_2O)	Locally produced, NIPH	Norway
Diva decloaker 10x	Biocare Medical	USA
Dimethyl sulfoxide	Merck	USA
Docosahexaenoic acid	Sigma-Aldrich	USA
Dinitrophenylhydrazine		
Eicosapentaenoic acid	Sigma-Aldrich	USA
El 808 Absorbance Reader	Biotek	USA
Eppendorf tubes 1.5 mL	VWR	USA
Excelsior ES	Life Technologies	USA
Formalin solution, neutral buffered, 10%	Sigma-Aldrich	USA
Hanks Saline Solution	Biochrom	Germany
Hemin	Sigma-Aldrich	USA
HNE-BSA Control	Cell Biolabs	USA
Hoechst 33342	Life Technologies	USA
Hydrogen peroxide 30%	Merck	USA
Image Lab 3.01	Bio-Rad	USA
Iron (II) sulfate heptahydrate	Sigma-Aldrich	USA
Methanol	Merck	USA

Microm HM 355S	Life Technologies	USA
Minifold® II *SRC* 072/0	Schleicher & Schuell	Germany
Mitotracker® Red CMH2kROS	Life Technologies	USA
Palmitic Acid	Sigma-Aldrich	USA
PAP-pen	VECTOR	USA
Phosphate buffered saline (PBS)	Locally produced, NIPH	Norway
Polysine slides	Life Technologies	USA
O-xylene	Sigma-Aldrich	USA
OxiSelect™ Protein Carbonyl ELISA Kit	Cell Biolabs	USA
S3023 Mounting Medium	Dako	USA
Sodium Chloride (NaCl)	Merck	USA
Sodium deoxycholate	Sigma-Aldrich	USA
SuperSignal™ West Dura Extended Duration Substrate	Life Technologies	USA
Tissue lyser II	QIAGEN	Germany
Trizma Hydrochloride	Sigma-Aldrich	USA
Tween 20	Bio-Rad	USA